SAPIENZA
UNIVERSITÀ DI ROMA

Tidal deformation of neutron stars

Facoltà di Scienze Matematiche, Fisiche e Naturali

Corso di Laurea in Fisica

Candidate

Andrea Sabatucci
ID number 1609795

Thesis Advisor

Prof. Omar Benhar Noccioli

Academic Year 2017/2018

Thesis not yet defended

Tidal deformation of neutron stars
Bachelor's thesis. Sapienza – University of Rome

© 2018 Andrea Sabatucci. All rights reserved

This thesis has been typeset by LaTeX and the Sapthesis class.

Version: November 3, 2018

Author's email: andrea.sabatucci1994@gmail.com

Dedicate to my family and friends

Contents

Abstract

The recently observation of a gravitational-wave signal emitted by an inspiraling binary neutron star system, made by the LIGO-VIRGO collaboration, opened up to the possibility of collecting new information about how matter behaves at the extreme conditions present inside a neutron star. During the inspiral, the information about the structure of the compact objects that make up the binary system, is mainly encoded in deformation effects due to tides and rotations. Tidal effects are governed by a dimensionless parameter expressing the ratio between the quadrupolar moment induced on a body by an external tidal field and the field itself: the tidal Love number. In this work of thesis we aid to compute the tidal Love number, relative to three different equations of state describing the neutron star matter at beta equilibrium. We employed a *Fortran 90* computational code, based on a fourth ordered Runge-Kutta algorithm, to integrate the equations of Tolman Oppenheimer and Volkoff that describe the structure of a stationary and spherically symmetric star, according to the theory of General Relativity. The three equations of state examined in this work are: a relativistic mean-field one, GM3; a nuclear many-body one, based on the formalism of correlated basis functions, CBF-EI; a model based on the extrapolation from measured nuclear properties, LS-bulk. We present here the calculation of the love number, spanning a wide range of the star's compactness parameter (M/R) and a discussion about the consistency of our results with the recently acquired data coming from the gravitational waves detection of a binary neutron stars merger made on 17 August 2017 by the LIGO-VIRGO detectors.

Introduction

Compact stars are believed to be the final stage of the stellar evolution and they are physically interesting because are composed by matter in very extreme conditions. Compact stars can be divided into three main categories: white dwarfs, neutron stars (NS) and black holes. Which of these three objects will arise at the end of the stellar evolution depends on the mass of the progenitor star.

White dwarfs represent one of the greatest success of quantum mechanics. Indeed they are sustained only by the degeneracy pressure of the electrons, that is a pure quantum effect.

Neutron stars are actually the most interesting objects, since they contains information concerning many different aspects of current physics. In neutron stars all the four fundamental interactions, i.e. gravity, electromagnetism, the weak and the strong forces, play a role. To understand the behavior of neutron stars are necessary notions of general relativity, high energy particle physics, condensed matter physics and statistical mechanics. The extreme conditions reached in the interior of neutron stars are impossible to reach with Earth-based experiments, therefore they represent our greatest laboratory in the Universe in order to understand the behavior of matter at so large energies.

Finally, black holes are the most mysterious objects in the Universe. Our knowledge about them is limited on the region outside their event horizon, since general relativity prohibits information to going out from this region. This made the interior of a black hole inaccessible to us. Actually it is currently believed that black holes aren't really black, thanks to the work of Stephen Hawking that carried out a very complex calculation in the framework of relativistic quantum fields theory, demonstrating that black holes emit a thermal radiation due exclusively to quantum effects, known as the Hawking radiation.

The main characters of this work of thesis will be the neutron stars. They, as already said, represent a great source of information for very different aspects of physics, but our knowledge about them is still very limited, in particular about what concern the most interior region, i.e. the core, where matter reaches densities very much larger than the density of saturation of atomic nuclei $\rho_0 = 2.67 \cdot 10^{14}\, g/cm^3$ that is the highest density achievable on Earth.

The main goal in understanding the behavior of matter in such an extreme environment is to carry out some predictions about macroscopic properties starting from a consistent treatment of the underlying microscopic dynamics. However in the NS interior the main contribute to the microscopic dynamics comes from the strong interactions that made very difficult an *ab initio* description based on the fundamental theory that rules such processes. Indeed strong interactions present

great mathematical difficulties, usually correlated with the impossibility to do a perturbative treatment. It is therefore necessary to rely upon approximations and theoretical models based on phenomenological considerations and constrained by the experimental observations. However, even following this approach there are troubles arising from the lack of empirical data. This is due to the fact that, as already said, simulating the interior of a neutron star is impossible in a laboratory, therefore the only data we have, come from astrophysical observations. The main purpose of the theoretical efforts in this field is therefore to propose a consistent way to model the microscopic dynamics in order to infer an equation of state (EOS) for the neutron star matter and use such EOS to carry out some astrophysical predictions that have to be confronted with experimental data.

The discover of the gravitational waves (GW) opened to the possibility of use their detection as a new source of information about neutron star's structure. There was several works that have shown how some equation-of-state dependent effects are accessible to measurement by the current generation of Earth-based gravitational-wave detectors (some of them are resumed in [1]). On 17 August 2017 the LIGO and VIRGO collaboration makes its first detection of a binary neutron star system (BNS) opening a new frontier of this kind of researches. It can be shown that the signal provided by the coalescence of two compact stars is affected, though weakly, by the equation of state of the component objects. These kind of effects are primarily due to tides and rotation that deform the bodies and consequently affect the shape of the detected gravitational-wave signal. For slow spinning stars the deformation effects have to be primarily ascribed to tidal effects.

In this work of thesis we examined three different EOS models, based on three different approaches, and we gave an estimate of how they would affect a gravitational-wave signal through tidal deformations. The effect of tidal deformations on the shape of a detected gravitational waveform is regulated by an dimensionless parameter the *tidal Love number*, that expresses the ratio between the multipole moment acquired by a body under the effect of an external tidal field, and the field itself. We took into consideration a quadrupolar deformation and therefore we computed the so called $l = 2$ tidal Love number, k_2, for the three EOSs studied.

The thesis is structured as follows. In chapter 1 we briefly review the main properties of white dwarfs, in order to introduce the reader to the study of the compact stars with an example that is currently well understood. In chapter 2 we introduce the neutron stars resuming their main properties that are believed to be well described by the existing models and the ones that are still not clear. At the end of this chapter we also briefly present two methods that can be used to infer an EOS governing the neutron star's matter. In chapter 3 we recap some useful features of general relativity and then we present the general relativistic stellar structure's equations firstly obtained by Tolman Oppenheimer and Volkoff (TOV). We also introduce the three EOSs examined in this work and the results we obtained using them to numerical integrate the TOV equations. In chapter 4 we introduce tidal effects, the theory of the tidal Love number, the method we used to compute it and our results. Finally in chapter 5 we draw our conclusions.

[AGGIUNGI NOTA SU UNITÀ DI MISURA, PRIMA DEVO METTERE IL LAVORO IN UNITÀ CONSISTENTI]

Chapter 1

White dwarfs

Compact stars, i.e. white dwarfs neutron stars and black holes, are believed to be the final stage of stellar evolution. Which of these three different objects would appear at the end of the lifetime of a star is triggered by the mass of the star itself. Observational data and theoretical calculations indicate that stars with a mass $M \lesssim 8M_\odot$[1] will end in a white dwarf, with typical mass, radius and density of respectively: $M \sim 1M_\odot$, $R \sim 5000\,km$ and $\bar{\rho} = 10^6\ g/cm^3$. Neutron stars or black holes are thought to be the leftover of the gravitational collapse following a supernova explosion of stars with a mass greater than $8M_\odot$, but it is still not clear which mechanism will produce one instead of the other [2]. Compact stars are different from the other stars, whose stability against gravitational collapse is due to thermal pressure. In this kind of stars, instead, the pressure needed to balance the self-gravity is provided by quantum effects and interactions between particles inside the object. In a white dwarf the main contribution comes from the electrons degenerate pressure. In this chapter we will focus on the main features of the white dwarfs. White dwarfs are the most well understood compact stars in the Universe, thus a good understanding of their physics is a necessary weapon to face the more intricate problems regarding the neutron stars, which will be the main characters of this work.

1.0.1 Euler equation of hydrostatic equilibrium

For the purpose of introduce the newtonian stellar structure equations, which will enable us to evaluate the astrophysical properties (such as mass, radius...) of a stationary spherically symmetric star in equilibrium, we first have to know a little of classical fluid dynamics. There are two principal point of views to describe the behavior of a classical fluid:

- the lagrangian specification: that consists in studying the evolution of each infinitesimal element[2] of the fluid as it was a point-like particle with its own equation of motion;

[1] $M_\odot$ denotes the mass of the sun that is $M_\odot = 1.9891 \cdot 10^{30}\,kg$

[2] When we talk about "infinitesimal" fluid element we are always talking about a mass element that is much smaller compared to the macroscopic dimensions of the fluid, but always big enough to contain a great number of particles, so all the quantities we relates to this fluid element can be thought as mean quantities with very little fluctuations.

- the eulerian specification: that is a field view of the fluid. In this framework one regards the meaningful quantities, such as velocity, as field quantities, assigning them a specific value in each point of the fluid at any given instant of time.

The two specifications are equivalent, and it's always possible to pass from one to the other depending on the problem one faces. The previous statement is equivalent to say that whenever knowing the quantity $\vec{r}(\vec{r_0}, t) \; \forall \; (t, \vec{r_0})$ (that means to resolve the Lagrangian problem), it's always possible to know $\vec{v}(\vec{r}, t)$, that is a field quantity. This is possible because the equations of classical dynamics are always deterministic, so one can always invert the relation $\vec{r}(\vec{r_0}, t)$ to $\vec{r_0}(\vec{r}, t)$ and define the quantity $\vec{v}(\vec{r}, t) = \dot{\vec{r}}(\vec{r_0}(\vec{r}, t), t)$.

We define also the Lagrangian derivative of an eulerian quantity as:

$$\frac{D}{Dt} = \vec{v} \cdot \vec{\nabla} + \frac{\partial}{\partial t} \tag{1.1}$$

where we did nothing but to apply the rule of composite derivatives.

Let us now consider a small mass element dM that leaves the volume V in the time dt. The mass element dM must be equal to the mass flux that passes over the surface Σ enclosing the volume V in the time dt. So we have the identity:

$$\frac{d}{dt} \int_V \rho(\vec{r}, t) dV' = - \int_{\Sigma(V')} \rho \vec{v} \cdot d\vec{S} \tag{1.2}$$

that, using the divergence theorem on the right hand side and passing the time derivative across the integral on the left hand side, leads to:

$$\frac{\partial \rho}{\partial t} = -\vec{\nabla} \cdot (\rho \vec{v}) = -\vec{v} \cdot \vec{\nabla} \rho - \rho \vec{\nabla} \cdot \vec{v} \tag{1.3}$$

finally using (1.1) we have:

$$\frac{D\rho}{Dt} = -\rho \vec{\nabla} \cdot \vec{v} \tag{1.4}$$

that is the continuity equation.

Let's consider a fluid element of volume V and now write down the second Principle of dynamics for the forces that act on it:

$$\frac{D(M\vec{v})}{Dt} = \vec{F_V} - \int_{\Sigma(V)} P d\vec{S} \tag{1.5}$$

where F_V is the resultat of the volume forces and P is the pressure due to the fluid surrounding the element V. $\vec{F_V}$ resumes all external forces that can be thought to be of the type:

$$- \int_V \tilde{\rho}(\vec{x}) \vec{\nabla} \Phi(\vec{x}) dV', \tag{1.6}$$

where $\Phi(\vec{x})$ is a generic potential and $\tilde{\rho}$ is a generic charge distribution (electric charge, mass ecc...). In our applications we will consider as volume forces only the gravitational one, so we can put $\tilde{\rho} = \rho$. If we also assume the incompressibility of the fluid, that is given by

$$\frac{D\rho}{Dt} = 0 \tag{1.7}$$

and use the vectorial identity

$$\int_{\Sigma(V)} f(\vec{x})d\vec{S} = \int_V \vec{\nabla} f(\vec{x})dV' \tag{1.8}$$

we can therefore write

$$\int_V dV' \frac{D(\rho\vec{v})}{Dt} = -\int_V dV'(\rho\vec{\nabla}\Phi + \vec{\nabla}P) \tag{1.9}$$

$$\Rightarrow \rho\frac{D\vec{v}}{Dt} + \frac{D\rho}{Dt}\vec{v} = -\rho\vec{\nabla}\Phi - \vec{\nabla}P \tag{1.10}$$

$$\Rightarrow \frac{D\vec{v}}{Dt} = -\vec{\nabla}\Phi - \frac{1}{\rho}\vec{\nabla}P. \tag{1.11}$$

This equation can be simplified taking into account the continuity equation, that together with the incompressibility condition leads to the constraint

$$\vec{\nabla}\cdot\vec{v} = 0. \tag{1.12}$$

We can also ignore the incompressibility condition and write the equation

$$\frac{D(\rho\vec{v})}{Dt} = -(\rho\vec{\nabla}\Phi + \vec{\nabla}P); \tag{1.13}$$

that is the so called Euler equation describing a perfect fluid in thermodynamical equilibrium. If we want to study the equilibrium configuration, (1.13) reduces to

$$\rho(\vec{x})\vec{\nabla}\Phi(\vec{x}) = -\vec{\nabla}P(\vec{x}). \tag{1.14}$$

Our initial purpose was to find the equations describing the structure of a star under its own gravity only. We treat a star as a spherically symmetric perfect fluid in hydrostatic equilibrium, i.e. we can use (1.14) in the simpler form resulting from imposing spherical symmetry

$$\frac{d\Phi(r)}{dr} = -\frac{1}{\rho(r)}\frac{dP(r)}{dr}. \tag{1.15}$$

Since Φ is the gravitational potential, it satisfies the Poisson equation:

$$\vec{\nabla}^2\Phi(\vec{x}) = 4\pi G\rho(\vec{x}), \tag{1.16}$$

that in the case of spherical symmetry becomes

$$\frac{1}{r^2}\frac{d}{dr}\left(r^2\frac{d\Phi(r)}{dr}\right) = 4\pi G\rho(r); \tag{1.17}$$

substituting the equation (1.15) into (1.17) and making some other manipulations we finally have:

$$\frac{dP}{dr} = -G\frac{M(r)\rho(r)}{r^2}; \tag{1.18}$$

$$M(r) = 4\pi\int_0^r r'^2\rho(r')\,dr'. \tag{1.19}$$

These are two differential equations with three unknown functions, so we need one more equation. For example, assuming $P = P(\rho)$, it may be sufficient to know the expression of $dP/d\rho$ to solve equations (1.18) and (1.19). This will be the topic of the next section.

1.0.2 Degenerate Fermi gas

We have already seen that in order to solve the stellar structure equations we need to know the relation $P(\rho)$, hence we have to know the equation of state (EOS) of the system we are studying. The equation of state is a nontrivial relation linking the independent thermodynamical variables that we need to specify the state of a physical system. We can imagine an equation of state as a relation of the type: $f(P, n, T) = 0$ where the independent variables are respectively: pressure, density of particles and temperature. In general, the EOS can be written as a power series of the pressure in function of n with temperature-dependent coefficients, known as virial expansion:

$$P = k_B nT(1 + nB(T) + n^2 C(T) + ...) \tag{1.20}$$

that, in the limit of small n, when we can keep only the first term of the series, reduces to the perfect gas law:

$$P = k_B \frac{N}{V} T. \tag{1.21}$$

In the equation of state are therefore encoded all the microscopic properties that characterize the system we are studying.

In this section we want to point out the main features of a system made up by free and non-interacting fermions, and we will find that the main contribution to the pressure of such a system is due to the Fermi exclusion principle. In the rest of this paragraph we will follow the treatment of [3][4]. Let us consider the free Hamiltonian of a single particle:

$$\hat{H}\phi(\vec{x}) = -\frac{\hbar^2}{2m}\vec{\nabla}^2\,\phi(\vec{x}). \tag{1.22}$$

We are interest in the eigenfunctions of $\hat{H}$, and since the system is translationally invariant, the identity

$$[\hat{H}, \hat{P}] = 0 \tag{1.23}$$

holds i.e. we can search the eigenfunctions of $\hat{H}$ among the ones of $\hat{P} = -i\hbar\vec{\nabla}$, that are:

$$\phi_p(\vec{x}) = Ne^{-i\frac{\vec{p}\cdot\vec{x}}{\hbar}} \tag{1.24}$$

where N is a normalization constant. It can be easily seen that (1.24) satisfies the eigenvalues equation for $\hat{H}$

$$\hat{H}\phi_p = \epsilon_p\,\phi_p \tag{1.25}$$

with eigenvalues

$$\epsilon_p = \frac{p^2}{2m}. \tag{1.26}$$

We now enclose the system in a cubic volume $V = L^3$ and impose periodic boundary conditions on $\phi(\vec{x})$[3]:

$$\phi(x, y, z) = \phi(x + L, y, z) = \phi(x, y + L, z) = \phi(x, y, z + L). \tag{1.27}$$

[3]We are in general interest on the bulk properties of such a system, so if we are dealing with a great number of particles in a big volume it seems reasonable to assume that the boundary condition doesn't affect the bulk of the system, we have so a general arbitrariness on making such a choice.

Since we enclosed the system in a finite volume V, the normalization constant N in (1.24) takes the value of $1/\sqrt{V}$, in order to fulfill the condition:

$$\int_V d^3x \, |\phi_p(\vec{x})|^2 = 1. \tag{1.28}$$

The boundary conditions (1.27), together with (1.24), imply that the ϕ_ps satisfies:

$$e^{-i\frac{p_i(x_i+L)}{\hbar}} = e^{-i\frac{p_i x_i}{\hbar}} e^{-i\frac{p_i L}{\hbar}} = e^{-i\frac{p_i x_i}{\hbar}} \tag{1.29}$$

$$\Rightarrow e^{-i\frac{p_i L}{\hbar}} = 1 \tag{1.30}$$

$$\Rightarrow k_i = \frac{p_i}{\hbar} = \frac{2\pi n_i}{L}, \;\; n_i \text{ integer}; \tag{1.31}$$

where the index i labels the generic component of a three dimensional vector. Equation (1.31) means that we are now dealing with a system characterized by a set of discrete states, which are labeled by three integer numbers (n_x, n_y, n_z). Thus in a three dimensional space with Cartesian axes k_x, k_y, k_z the allowed wave vectors $(\vec{k})$ are those whose coordinates along the three axes are given by integral multiples of $2\pi/L$ (this situation for the two-dimensional case is illustrated in Fig. 1.1 taken from [3]). However, the description of the states of a real physical particle, in order to be

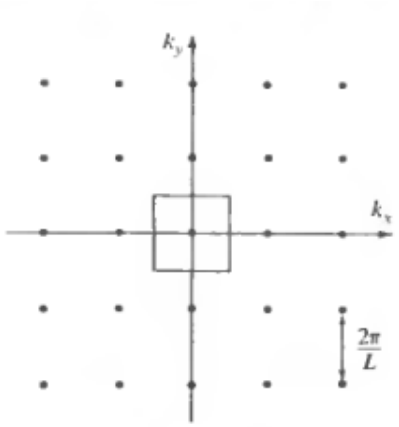

Figure 1.1. Points in a two-dimensional k-space of the form $k_x = 2\pi n_x/L$, $k_y = 2\pi n_y/L$. Note that the volume per point is $(2\pi/L)^2$, whereas for a d-dimensional lattice it will be of $(2\pi/L)^d$

complete, needs the additional information regarding its spin orientation; since the Hamiltonian of a free particle doesn't affect its spin, we can choose an eigenfunction of $\hat{H}$ of the form:

$$\psi_{p,s}(\vec{x}) = \phi_p(\vec{x}) \, \chi_s; \tag{1.32}$$

where χ_s satisfies

$$\hat{S}_z \, \chi_s = \hbar s \, \chi_s \tag{1.33}$$

with $s = \pm(1/2)$, since we usually are are dealing with electrons. As we already said at the beginning, we want to describe a system of N fermions, so we wish to know the energy levels of a many-particle system. Nevertheless we are interest in a

non-interacting problem, so under this assumption, we can take as eigenfunctions of the total Hamiltonian ($\hat{H}_{tot} = \sum_{i=1}^{N} \hat{H}_i$) a tensor product of N eigenfunctions of the single-particle Hamiltonian, being careful in taking only all those combinations that are compatible with the Pauli exclusion principle. We can now easily build up the ground state of such a system by simply placing one, and only one, fermion in each single particle state, and then filling all the one-particle energetic levels from the bottom ($E = 0$) until we end the particles. The one-fermion levels (1.32) are specified by the wave vector $\vec{k}$ (related to $\vec{p}$ from (1.31)) and by the projection of its spin along an arbitrary axes; therefore associated with each $\vec{k}$ there are two fermion states, one associated to each spin polarization. Since the energy of a one-particle level is directly proportional to the square of its wave vector, when N is enormous the occupied region in k-space will be indistinguishable from a sphere. If we want to know the radius of that sphere, we need to know the relation that links the number of allowed states with the volume of the k-space region they occupy. In this case, as in many other cases like this, we needs to know how many $\vec{k}$ are contained in a region of k-space that is enormous on the scale of $2\pi/L$ and that therefore contains a vast number of allowed points. If the region is very large, and not too irregularly shaped (so that only a negligible fraction of the points are within $O(2\pi/L)$ of the surface) the number of allowed points is just the volume of the allowed region divided by the volume per point in the network of the allowed values of $\vec{k}$. Thus we can conclude that the number of points contained in a region of volume Ω of k-space is:

$$\frac{\Omega}{(2\pi/L)^3} = \frac{\Omega V}{(2\pi)^3}; \tag{1.34}$$

or alternatively that the density of points in k-space per unit volume is just:

$$\frac{V}{8\pi^3}. \tag{1.35}$$

If we call k_F (F for Fermi) the radius of the sphere of allowed k-points for a free particle system, we obtain, using (1.34) and $\Omega = \frac{4}{3}\pi k_F^3$:

$$\frac{N}{2} = \frac{4/3\pi k_F^3 V}{(2\pi)^3} = \frac{V}{6\pi^2} k_F^3; \tag{1.36}$$

i.e.

$$k_F = \left(3\pi^2 n\right)^{\frac{1}{3}}, \quad n = \frac{N}{V}. \tag{1.37}$$

In equation (1.36) N is the number of particles and the denominator 2 comes from the spin degeneration of each $\vec{k}$ state.

We can now evaluate the total energy E_0 of the ground state of this N-particle system:

$$E_0 = \sum_{p<p_F} \frac{p^2}{2m}. \tag{1.38}$$

In order to evaluate (1.38) we use the following property: let $F(\vec{k})$ be a function that varies very little on the scale given by $\Delta\vec{k}$; since in the limit of $\Delta\vec{k} \to 0$ the sum $\sum_{\{k\}} F(\vec{k})\Delta\vec{k}$ approaches the integral $\int d\vec{k}\, F(\vec{k})$, we can use the approximation:

$$\frac{1}{\Delta\vec{k}} \sum_{\{k\}} F(\vec{k})\Delta\vec{k} \approx \frac{1}{\Delta\vec{k}} \int d\vec{k}\, F(\vec{k}). \tag{1.39}$$

Combining (1.31) and (1.39), and using $\Delta\vec{k} = 8\pi^3/V$ (1.38) reduces to:

$$E_0 = 2\sum_{k<k_F} \frac{\hbar^2 k^2}{2m}\frac{\Delta\vec{k}}{\Delta\vec{k}} = \frac{V}{(2\pi)^3}2\sum_{k<k_F}\frac{\hbar^2}{2m}k^2\Delta\vec{k} \approx \frac{V}{(2\pi)^3}2\int_{k<k_F}\frac{\hbar^2}{2m}k^2\,d\vec{k} \quad (1.40)$$

$$\Rightarrow \frac{E_0}{V} = \frac{\hbar^2}{m}\frac{k_F^5}{10\pi^2}. \quad (1.41)$$

Equation (1.41) represents the energy density of a quantum system, made up by N non-interacting fermions of mass m and spin 1/2, in its ground state (thus, from a thermodynamical point of view, at zero temperature). A gas like that in its ground state is said to be *fully degenerate*. At this point, using equations (1.37) and (1.41), and defining $\epsilon_F = (\hbar k_F)^2/2m$, we can point out the following expressions for the energy density and energy per particle at $T = 0$:

$$\frac{E_0}{V} = \varepsilon = \frac{3}{5}n\epsilon_F; \quad (1.42)$$

$$\frac{E_0}{N} = e = \frac{3}{5}\epsilon_F. \quad (1.43)$$

We can now use the thermodynamical relation:

$$P = -\left(\frac{\partial E}{\partial V}\right)_N, \quad (1.44)$$

to find the value of the pressure P that result to be[4]

$$P = \frac{2}{3}\frac{E_0}{V}. \quad (1.45)$$

All we did until now holds for a gas that is fully degenerate i.e. at
$T = 0°\,K$; nevertheless we know that the temperature in the star interior is far above this limit. Let us now discuss if, and so in which cases, the approximation of a fully degenerate gas can be used to well describe the matter inside a white dwarf. If we consider a classical system of N non-interacting particles, we can apply the equipartition theorem to find the mean energy of the system at temperature T:

$$\langle E\rangle = \frac{3}{2}Nk_BT. \quad (1.46)$$

From eq. (1.42) comes that the energy in the ground state, that is entirely due to the degeneracy energy of the fermions is :

$$E_0 = \frac{3}{5}N\epsilon_F. \quad (1.47)$$

According to (1.46) and (1.47) we can assume that full degeneracy occurs when $E_0 >> \langle E\rangle$ i.e. k_BT is much smaller than the Fermi energy ϵ_F. Because

$$\epsilon_F = \frac{\hbar^2 k_F^2}{2m}, \quad (1.48)$$

[4]In deriving eq. (1.45) one have to remember that the arguments of E must be S, V and N, where, since we are dealing with a system in its ground state, we can put S=0.

using (1.37) we find that the limit of fully degeneracy holds when:

$$\epsilon_F = \frac{\hbar^2}{2m}(3\pi^2 n)^{\frac{2}{3}} >> k_B T \tag{1.49}$$

$$\Rightarrow n >> n_0 = \frac{1}{3\pi^2}\left(\frac{2mk_BT}{\hbar^2}\right)^{\frac{3}{2}}. \tag{1.50}$$

Therefore, if in the white dwarf's interior the density of the fermions reaches a value that is far above the value of n_0 at the typical temperature of the star, we can consider effectively the matter inside the star to be fully degenerate. For an ordinary star at the stage of hydrogen burning, like the Sun, the interior temperature is $\sim 10^7\ K$, and the corresponding n_0 turns to be $\sim 10^{26}\, cm^{-3}$. If we assume that all the electrons come from a fully ionized hydrogen gas, the matter density of the proton-electron plasma is

$$\rho = (m_p + m_e)n_0 \sim 200\, g/cm^3, \tag{1.51}$$

with m_p being the mass of the proton ($m_p = 1.673 \times 10^{-24}\, g$). This density can be high for stars in the early phase of hydrogen burning, but for aged stars that have developed a substantial helium core the density ($m_n = 1.675 \times 10^{-24}\, g \sim m_p$ denotes the mass of the neutron)

$$\rho = (m_n + m_p + m_e)n_0 \sim 400\, g/cm^3, \tag{1.52}$$

can be easily be exceeded within core. In the core of a white dwarf typical densities reach the order of $\sim 10^7\, g/cm^3$. As a consequence the thermal energy can be safely neglected and the primary contribution comes from the degeneracy energy.

As final remark we note that, combining equations (1.41) and (1.45) we find that :

$$P = \frac{2}{3}\frac{\hbar^2}{m}\frac{k_F^5}{10\pi^2}. \tag{1.53}$$

In eq. (1.53) we note that the dependence of the pressure on the type of particle we are dealing with, is carried only by the mass in the denominator; therefore the degeneracy pressure due, for example, to electrons is ~ 2000 times bigger than the one of the nucleons at the same numerical density.

In the previous discussion we made the tacit assumption that the system was made up by non-relativistic particles. However we saw how the properties of the system depend primarily from the distribution of quantum states, which is dictated by translational invariance only that continues to hold even if we replace the single particle hamiltonian with a pure relativistic one. Therefore we conclude that relaxing the non-relativistic hypothesis has the only consequence of replacing the non-relativistic energy with its relativistic counterpart:

$$\frac{p^2}{2m} \rightarrow \sqrt{p^2c^2 + m^2c^4} - mc^2. \tag{1.54}$$

The transition to the relativistic regime occurs when the kinetic energy of the particle becomes comparable with the energy associated with its rest mass, m. Therefore it is possible to define a critical density n_c such that for $n << n_c$ the system is in the

non-relativistic regime, while for $n >> n_c$ the system approaches the ultra-relativistic regime. This critical density can be find imposing the equality between the Fermi energy and the rest energy of the particle that leads to:

$$n_c = \frac{2^{3/2}}{3\pi^2}\left(\frac{mc}{\hbar}\right)^3; \tag{1.55}$$

that, in the case of electrons, takes the value $n_c \sim 1.6 \times 10^{30} cm^{-3}$.

We can now calculate the energy density and pressure that result to be:

$$\varepsilon = 2\frac{1}{h^3}4\pi \int_0^{p_F} dp\, p^2 \left[\sqrt{p^2c^2 + m^2c^4} - mc^2\right]; \tag{1.56}$$

$$P = \frac{2}{3}\frac{1}{h^3}4\pi \int_0^{p_F} dp\, p^2 \left(p\frac{\partial \epsilon_p}{\partial p}\right). \tag{1.57}$$

In eq. (1.57) we defined the pressure as the momentum flux on a surface of the cubic volume V due to a single particle:

$$P(p_i) = \frac{1}{L^2}\frac{dp_i}{dt} = np_iv_i = np_i\frac{\partial \epsilon_p}{p_i} = \frac{1}{3}\frac{N}{V}p\frac{\partial \epsilon_p}{\partial p}; \tag{1.58}$$

and then integrated over all allowed p. The last equality in equation (1.58) follows from spatial isotropy.[5] Naturally we will obtain the same result for the pressure using the thermodynamical relation as we did before for the non-relativistic case. Carrying out the integrals from equations (1.56) and (1.57) we have:

$$\varepsilon = \frac{\pi m}{\lambda^3}\left[t(2t^2+1)\sqrt{t^2+1} - ln\left(t + \sqrt{t^2+1}\right) - \frac{8t^2}{3}\right], \tag{1.60}$$

$$P = \frac{\pi m}{\lambda^3}\left[\frac{1}{3}t(2t^2-3)\sqrt{t^2+1} + ln\left(t + \sqrt{t^2+1}\right)\right]; \tag{1.61}$$

where $\lambda = h/mc$ is the particle Compton wavelength and

$$t = \frac{p_F}{m} = \frac{1}{m}(3\pi^2 n)^{1/3}. \tag{1.62}$$

Finally, since we want to use the theory of fully degenerate gas to describe the behavior of matter inside a white dwarf, we have to justify the approximation of non-interacting particles. In this sense we now discuss the possible relevance of electrostatic interactions. We can roughly estimate them, noting that their energy can be write as:

$$E_c = Z\frac{e^2}{\langle r \rangle} \propto Z\, e^2\, n^{1/3} \tag{1.63}$$

[5] As the system is isotropic we have that

$$p_iv_i = \frac{1}{3}\sum_{i=1}^{3} p_iv_i = \frac{1}{3}(\vec{p}\cdot\vec{v}) = \frac{1}{3}\left(\vec{p}\cdot\vec{\nabla}_p\,\epsilon_p\right) = \frac{1}{3}p\frac{\partial \epsilon_p}{\partial p}. \tag{1.59}$$

where Ze is the electric charge of the ions and $\langle r \rangle$ denotes the typical electron-ion separation distance that is proportional to $1/n^{1/3}$. It follows that the ratio between the Coulomb energy and the Fermi energy satisfies this proportionality relation:

$$\frac{E_c}{\epsilon_F} \propto \frac{1}{n^{1/3}}, \tag{1.64}$$

therefore for high numerical densities, how it happens in the white dwarf's interior, we can neglect the electrostatic contribution to the energy and treat safely the electrons as a fully degenerate Fermi gas.

1.1 Equation of state of a degenerate electron gas

In the previous section we have summarized the main properties of a degenerate Fermi gas. We also pointed out how, in the environment of the white dwarfs interior, we can consider the pressure as due to electron degeneracy only, because the thermal one, as the one provided by the degeneracy of nucleons, becomes negligible. Now we are interest to point out the equation of state (EOS) of such a system. After doing that we will have everything we need to integrate the stellar structure equations. We are therefore searching for a relation such as $P = P(\rho)$. If we define as Y_e the number of electrons per nucleon, being $m_p \sim m_n$ the mass of a nucleon and m_e the mass of the electron, we have this relation linking the matter density ρ to the electron number density n_e:

$$\rho = \frac{m_p}{Y_e} n_e + m_e n_e \approx \frac{m_p}{Y_e} n_e. \tag{1.65}$$

Onece we have (1.65), the EOS we are looking for can be successfully provided by integration of the (1.57). Nevertheless this integral results to be very complex, so it is useful to consider it in two different significant regimes that leads to simple approximations: the non-relativistic and the ultra-relativistic ones. This two limits occurs respectively when the kinetic energy of the particle is much smaller then the energy at rest. The last statement is implemented in the (1.57) imposing respectively either $p_F << mc$ or $p_F >> mc$. Therefore, since p_F is the maximum value of the momentum, for the non-relativistic case we have, see eq.(1.57):

$$P = \frac{2}{3}\frac{1}{h^3} 4\pi \int_0^{p_F} dp\, p^3 \frac{pc^2}{\sqrt{p^2c^2 + m^2c^4}} = \frac{2}{3}\frac{1}{h^3} 4\pi \int_0^{p_F} dp\, \frac{p^4}{m} \frac{1}{\sqrt{1 + \frac{p^2}{m^2c^2}}} \tag{1.66}$$

$$= \frac{2}{3}\frac{1}{h^3} 4\pi \int_0^{p_F} dp\, \frac{p^4}{m} \left(1 + O\left(\frac{p^2}{m^2c^2}\right)\right) \approx \frac{2}{3}\frac{1}{h^3} 4\pi \int_0^{p_F} dp\, \frac{p^4}{m} \tag{1.67}$$

$$= \frac{8\pi}{h^3 m} \frac{p_F^5}{15} = \frac{\hbar^2}{15\pi^2 m} \left(3\pi^2 n\right)^{\frac{5}{3}}. \tag{1.68}$$

Equation (1.68) is, as expected, equal to (1.53). Finally using eq. (1.65) we point out the EOS for a non-relativistic fully degenerate gas of electrons in the form $P(\rho)$:

$$P(\rho) = \frac{\hbar^2}{15\pi^2 m} \left(3\pi^2 \frac{Y_e}{m_p}\right)^{\frac{5}{3}} \rho^{\frac{5}{3}}. \tag{1.69}$$

Following a similar approach we can equivalently point out the EOS relative to the ultra-relativistic regime:

$$P(\rho) = \frac{\hbar c}{12\pi^2}\left(3\pi^2\frac{Y_e}{m_p}\right)^{\frac{4}{3}}\rho^{\frac{4}{3}}. \tag{1.70}$$

An equation of state that can be written in the form

$$P \propto \rho^{\Gamma}, \tag{1.71}$$

is said to be *polytropic*. The exponent Γ is called *adiabatic index*, whereas the quantity n, defined through:

$$\Gamma = 1 + \frac{1}{n} \tag{1.72}$$

is called *polytropic index*.

The adiabatic index, whose definition for a generic equation of state is

$$\Gamma = \frac{d(\ln P)}{d(\ln \rho)}, \tag{1.73}$$

is related to the compressibility χ of the system, characterizing the change of pressure with volume according to

$$\frac{1}{\chi} = -V\left(\frac{\partial P}{\partial V}\right)_N, \tag{1.74}$$

through

$$\Gamma = \frac{1}{\chi P}. \tag{1.75}$$

The compressibility is also related to the speed of sound in matter, c_s, defined as

$$c_s^2 = \left(\frac{\partial P}{\partial \rho}\right) = \frac{1}{\chi\rho}. \tag{1.76}$$

The magnitude of the adiabatic index reflects the *stiffnes* of the EOS: larger stiffness correspond to more incompressible matter.

Summing up, the most important aspect that comes from these last two sections is that we can write the EOS of a degenerate Fermi gas in two notable regimes, non-relativistic and ultra-relativistic, as an equation of the form:

$$P(\rho) = K\rho^{\Gamma}, \tag{1.77}$$

where Γ assumes the values of $5/3$ and $4/3$ respectively for the two cases. We now have all the necessary to integrate the stellar structure equations.

1.2 Structure of white dwarfs

We can now write down the stellar structure equation for a white dwarf in the two regimes in which we derived the EOS:

$$\begin{cases} \frac{dP}{dr} = -G\frac{M(r)\rho(r)}{r^2} \\ M(r) = 4\pi\int_0^r r'^2\rho(r')\,dr' \\ P(\rho) = K\rho^{\Gamma} \end{cases} \tag{1.78}$$

where K is a constant and $\Gamma = 5/3$ and $4/3$ respectively for the non-relativistic and the ultra-relativistic regime. Equations (1.78) can now be integrated for any given value of the central density ρ_c, however, for brevity, we will not report the analytical solution (that can be found in [2]). We limit ourselves to say that equations (1.78) reduce to Lane-Emden equation, whose integration with adiabatic index $\Gamma = 5/3$ yields the relation:

$$M = 2.79 \cdot Y_e^2 \left(\frac{\rho_c}{\bar{\rho}}\right)^{\frac{1}{2}} M_\odot, \tag{1.79}$$

where $\bar{\rho}$ denotes the matter density corresponding to the critical density given by (1.55) for the case of electrons. The values resulting from this equation are in good agreement with astronomical observations, however we must note that the Lane-Emden equation doesn't predict an upper bound for the mass of stable with dwarfs. In 1931 Chandrasekhar pointed out that that the non-relativistic treatment was not longer justified. Therefore by replacing the EOS with its relativistic counterpart, Chandrasekhar predicted the existence of a maximum value of the mass for a white dwarf.

The existence of a critical mass can be understood also from qualitative considerations (see [2]). The equilibrium condition for a generic mass configuration imposes that the gradient of pressure is balanced by the gravitational attraction. Qualitatively, for the non-relativistic case:

$$P \sim \rho^{\frac{5}{3}} \rightarrow P \sim \frac{M^{\frac{5}{3}}}{R^5} \rightarrow \frac{dP}{dr} \sim \frac{M^{\frac{5}{3}}}{R^6}. \tag{1.80}$$

Alternatively, for the ultra-relativistic case:

$$P \sim \rho^{\frac{4}{3}} \rightarrow P \sim \frac{M^{\frac{4}{3}}}{R^4} \rightarrow \frac{dP}{dr} \sim \frac{M^{\frac{4}{3}}}{R^5}. \tag{1.81}$$

The gravitational force per unit volume behaves like:

$$\frac{Gm(r)\rho}{r^2} \sim \frac{M^2}{R^5}. \tag{1.82}$$

Since the equation for hydrostatic equilibrium requires

$$\frac{dP}{dr} = -\frac{Gm(r)\rho}{r^2}, \tag{1.83}$$

we can draw the following conclusions. In the non-relativistic case the dependence on R of the pressure gradient and the gravitational force is different, so for each value of the mass we can in principle adjust the radius R such that eq. (1.83) holds. Alternatively in the ultra-relativistic case we have the same dependence on R in both sides, thus, since the dependence on M is different, the equilibrium is possible for one value of the mass only i.e. the critical mass.

1.3 A first test on the computational code

In order to extract our main results for the the neutron stars, we will make use, in the following of a computational code that is written in *Fortran90*. This code

enable us to integrate the relativistic stellar structure equations, known as the equations of Tolman Oppenheimer and Volkoff, that will be derived in the next chapters, for a generic equation of state given in input. Such a code employs a fourth ordered Runge-Kutta algorithm in order to integrate a system of differential equations. Before going on we report some results derived using a similar code for the integration of the non-relativistic stellar structure equations given by (1.78) with a polytropic EOS. We remark that the integration was carried out on the variable r and it was employed a variable integration step in order to accommodate strongly variable functions. Such a step is given by:

$$\Delta r = \Delta \cdot \left(\frac{1}{M} \frac{dM}{dr} - \frac{1}{P} \frac{dP}{dr} \right)^{-1} , \tag{1.84}$$

where Δ is an arbitrary scale parameter, that we usually put to $\Delta = 0.01$ as it was good compromise to maximize the efficiency. I report in the follows the results for the mass in function of the central density in the two significant regimes analyzed below. For the non-relativistic regime we integrated the equations (1.78) with a central density ranging from $\sim 10^4$ to $\sim 10^6\ g\, cm^{-3}$ and obviously $\Gamma = 5/3$. The constant K is given by eq. (1.69). In Fig. 1.2(a) is reported the resulting plot for $M/M_\odot$ in function of the central density ρ_c. In order to test its resemblance with the relation (1.79) it was performed a fit with the function $f(x) = A \cdot x^{1/2}$ that matched perfectly the sample.

I also performed the integration in the relativistic regime, with a central density range spanning from $\sim 10^8$ to $\sim 10^{10}\ g \cdot cm^{-3}$. The result for the $M/M_\odot$ vs ρ_c can be seen in Fig. 1.2(b)[6]. In this case the ratio $M/M_\odot$ is constant and equal to $M/M_\odot = 1.431$. The fact that the mass is constant for the ultra-relativistic case is in agreement with what has been said about the Chandrasekar observations concerning the existence of a limiting mass that he found to be [2]

$$M_{Chand} = 1.435\, M_\odot \tag{1.85}$$

.

[6]I performed the integration for the two different regimes employing density ranges where it is expected that the real EOS approaches the ones considered here, however the consideration i drew in this paragraph are independent on the density range, since i limit myself to point out the form of the function $M(\rho_c)$ that depends only from the EOS employed.

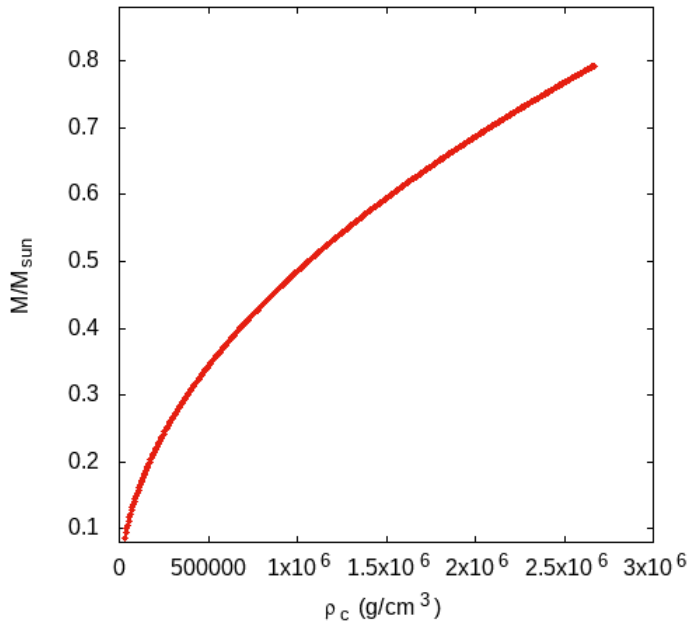

(a) non-relativistic regime

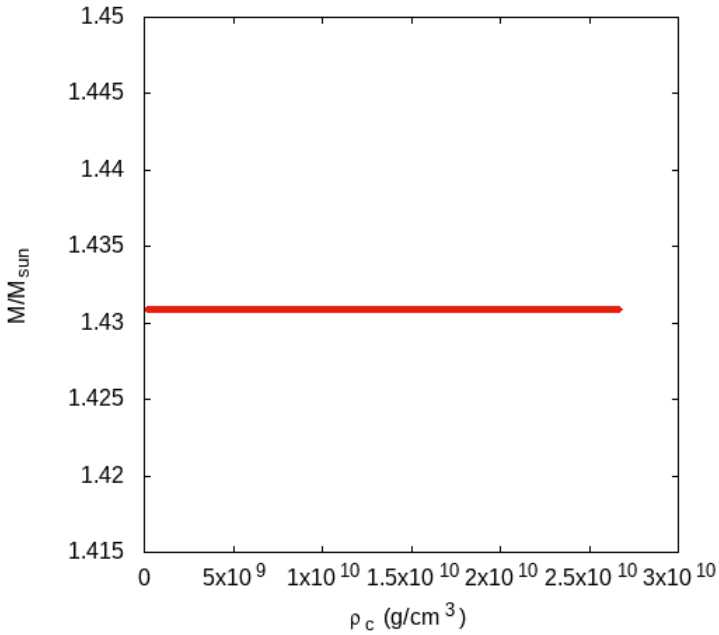

(b) ultra-relativistic regime

Figure 1.2. The results for the $M(\rho_c)$ function provided by the integration of the stellar structure equations in the non-relativistic regime (a) and in the ultra-relativistic one (b).

Chapter 2

Neutron stars

It was already mentioned that during the central phase of its evolution, the pressure needed to balance the gravitational contraction of a star is provided by the thermonuclear reactions that happen in its own core. When the fuel is all burnt out there is nothing which is opposed to self-gravity and the star collapses. As the contraction goes on the temperature increases and if the mass of the core is high enough, new thermonuclear reactions, which burn the heavier elements produced in the previous phase, sets in and a new equilibrium in reached. The thermonuclear evolution of a star goes on until the formation of the heavier element that is allowed by the star initial mass. As we said in the previous Chapter, for progenitor masses $\lesssim 8M_{\odot}$, according to current theories, the collapse proceeds until is halted by the degeneracy pressure of the electrons. The outer layers of the stars are then expelled as solar wind giving birth to a white dwarf. White dwarfs are usually composed by oxygen and carbon. If the progenitor mass is in the range $\sim 8 - 10\, M_{\odot}$ oxygen-neon-magnesium stars can form, but they are quite rare. White dwarfs can exist in stable configurations only if their mass is smaller then the Chandrasekhar limit, $M_{CH} \sim 1.4\, M_{\odot}$.

If the mass of the progenitor belongs to the range $\sim 8M_{\odot} < m < 20 - 30M_{\odot}$ the evolution follows a different path. Nuclear processes are able to burn elements heavier then carbon and oxygen, and exothermic nuclear reactions can proceed until the production of ^{56}Fe, which is the most stable element in nature[1].

The process which produce the iron core starts with silicon burning and goes through these stages:

$$^{28}Si +^{28} Si \rightarrow^{56} Ni + \gamma \tag{2.1}$$

$$^{56}Ni \rightarrow^{56} Co + e^{+} + \nu_e \tag{2.2}$$

$$^{56}Co \rightarrow^{56} Fe + e^{+} + \nu_e. \tag{2.3}$$

In addition to the appearance of the ^{56}Fe, the above process produces neutrinos that interact very little with the surrounding matter and thus go away from the star bringing out a relevant fraction of energy. Moreover, as the core density increases, the inverse β decay (electronic capture),

$$e^{-} + p \rightarrow n + \nu_e, \tag{2.4}$$

[1]No element heavier then ^{56}Fe can be generated by nuclear fusion of lighter elements through exothermic reactions.

that contributes to the production of neutrinos and therefore subtracts energy from the star, becomes more and more efficient. Other than the production of neutrinos, electronic capture tends to increase the number of neutrons, therefore heavier elements than ^{56}Fe may be produced through neutron capture, that is an endothermic process. Finally there is another endothermic reaction, known as photodisintegration that may take place. It is ignited by high energy photons ($> 8MeV$) and occurs as

$$\gamma +^{56} Fe \rightarrow 13\,^{4}He + 4n. \tag{2.5}$$

All these processes have the effect of decreasing the kinetic energy and thus the pressure inside the core, they therefore tend to destabilize the star. When the mass of the core exceeds the Chandrasekar limit it collapses within a fraction of second, reaching densities $\sim 10^{14} g/cm^3$ i.e. comparable with the central density of atomic nuclei $\rho_0 = 2.67 \cdot 10^{14} g/cm^3$. At this stage the core behaves as a giant nucleus, made mostly of neutrons and reacts elastically to further compression, producing a shock wave which ejects a significant fraction of matter in the outer layers of the star in a spectacular explosion. This phenomenon is called *supernova explosion*: the luminosity of the star suddenly increases to values exceeding the luminosity of the Sun ($L_\odot$) by a factor $\sim 10^9$, and elements heavier than ^{56}Fe are created. The remnant of this explosion is a nebula, in the middle of which sits the remnant of the core i.e. a *neutron star*.

Neutron stars are often observed as *pulsars*, i.e. radio sources whose emission exhibits a very sharp periodicity, blinking on and off at a constant frequency. This periodicity is due to the fact that pulsars are rapidly rotating objects whit strong magnetic fields ($B \sim 10^{11} - 10^{13}\, Gauss$) which emit beams of radio waves from the magnetic poles, that are not aligned with the rotation axis. The beam is clearly visible only when it points on the direction of the detectors.

There was a pioneering study, carried out in 1939 by Oppenheimer and Volkoff, within the framework of general relativity, concerning the structure of neutron stars. This work shows that the mass of a star made up by non-interacting neutrons cannot exceeds $\sim 0.8 M_\odot$. However, observed neutron stars masses was much bigger than this theoretical limit, pointing out that neutron star equilibrium requires a pressure other than the degeneracy one, the origin of which has to be ascribed to hadronic interactions.

Unfortunately, the need of including dynamical effects in the EOS collides with the complexity of the fundamental theory of strong interactions. As a consequence, all available description of the EOS of neutron star matter are obtained within theoretical models of the underlying dynamics and as much as possible constrained by empirical data.

In the following of this chapter we will give an overview of the believed internal structure of neutron stars.

2.1 Internal structure of neutron stars

Despite there are many different approaches trying to describe the behavior of neutron stars matter, under certain density ranges they predict more or less the same

properties. Therefore we can draw a general model for the neutron stars interior.

The internal structure of neutron stars is believed, as shown in figure 2.1, to be composite of a sequence of layers of different composition and density.

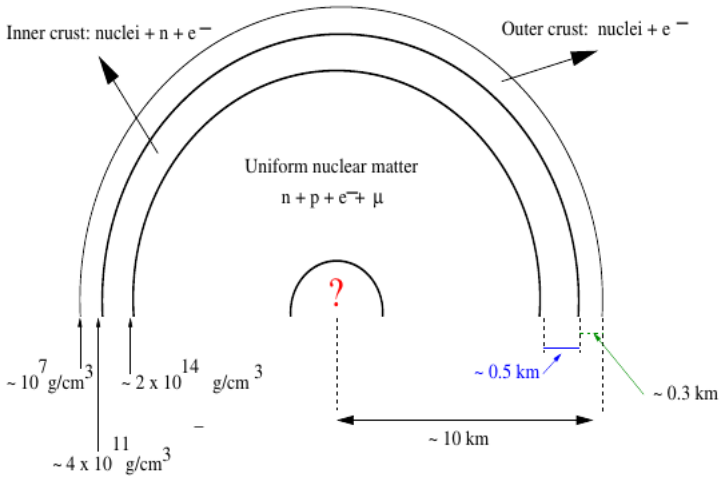

Figure 2.1. Schematic illustration of the believed neutron star section.

Proceeding from the exterior, we first encounter an outer crust, $0.3\,km$ thick, an inner crust, $\sim 0.5\,km$ thick and a core that extends over $10\,km$.

The density of the neutron star core ranges between $\sim \rho_0$ $(= 2.67 \cdot 10^{14} g/cm^3)$ at the boundary with the inner crust, and a central value that can be as large as $1 \div 4 \cdot 10^{15}\, g/cm^3$. All models of EOS based on hadronic degrees of freedom predict that in the density range $\rho_0 < \rho < 2\rho_0$ neutron star matter consists mainly of neutrons together with a small fraction of proton, electrons and muons, which is determined by the requirements of β equilibrium and charge neutrality. This picture may change significantly at larger densities with the appearance of heavy strange baryons produced by weak interactions, such the Σ^-, provided by:

$$n + e^- \rightarrow \Sigma^- + \nu_e, \tag{2.6}$$

that is energetically allowed when the sum of electron and neutron chemical potential equals the one of Σ^-.

Finally, as nucleons are known to be compact objects of size $\sim 0.5 - 1.0\, fm$ i.e. of density $\sim 10^{15}$, one could expect that whenever matter reaches this density a transition to a new phase takes place, leading to a situation in which quarks are no longer confined into hadrons.

In the description of neutron star interior we shall assume that the temperature is $T = 0$ and that matter is transparent to neutrinos. The first assumption is justified because the observed temperature of neutron stars reaches at least $T \leq 10^9\, K$, whereas the Fermi temperature of neutrons $(T_F = \epsilon_F / k_B)$ at the typical densities of neutron stars reaches $\sim 3 \cdot 10^{11} - 10^{12}\, K >> 10^9\, K$. The second assumption follows from the fact that the mean free path of neutrinos in nuclear matter at temperature $T \leq 10^9\, K$ is much larger than the typical radius of neutron stars.

2.1.1 The outer crust

The outer crust corresponds to densities ranging from $\sim 10^7\, g/cm^3$ to $\rho_d = 4 \cdot 10^{11}\, g/cm^3$. It is a solid layer composed by a lattice of heavy nuclei immersed in an electron gas. Proceeding toward the star interior, as density increases, the inverse β decay becomes more and more efficient, thanks to the increasing Fermi momentum of the electron gas that shifts the energy balance. As a result a large number of neutrons are produced in the density region $10^7 - 10^{11}\, g/cm^3$ and new nuclear species appear through the sequence:

$$Fe \rightarrow Ni \rightarrow Se \rightarrow Ge. \tag{2.7}$$

This process is called *neutronization*. In this region the pressure is mainly due to the degenerate electron gas. When the density approaches the so called neutron drip density, ρ_d, all nuclear bound states available for neutrons are filled, therefore they can no longer live bound to nuclei and start to leaking out. This effect is just called *neutron drip*.

2.1.2 The inner crust

In this region density ranges between ρ_d and $\rho_0 = 2.67 \cdot 10^{14}\, g/cm^3$. As already said, in this regime, since neutrons created by electron capture begins to drip out of the nuclei, the ground state corresponds to a mixture of two phases: matter consisting in neutron rich nuclei which contains in addition the relevant fraction of protons (therefore it is called Proton Rich Matter, PRM), and a neutron gas (NG). In addition there is the electron gas to ensure charge neutrality. The fundamental state of matter in this region is affected by the density of the two phases ρ_{PRM} and ρ_{NG}, the proton fraction in PRM and by the geometrical properties of the structures that are formed by the two phases which strongly depend on surface effects at the interface of different phases. Recent studies suggest that at densities $\rho_d < \rho < 0.35\rho_0$ the PRM is arranged in spheres, surrounded by a gas of electrons and neutrons. For higher densities the separation between spheres decreases up to the touching limit. At density of $0.35\rho_0 < \rho < 0.5\rho_0$ therefore the spheres merge forming bar-type structures, and for $0.5\rho_0 < \rho < 0.56\rho_0$ bars merge to form slab-type structures. When the density reaches the nuclear density ρ_0 the two phases form an homogeneous fluid of protons, neutrons and electrons.

There is a quite general consensus on the equation of state of matter in the crust because at such densities the properties of matter can be obtained by experimental data on neutron rich nuclei. Conversely the higher densities characterizing the core are unachievable in laboratory, therefore we have to rely on purely theoretical models only partially constrained by empirical data. In the next sections we will try to explain how such a model can be built up, giving particular attention to those one that was employed for the ultimate purpose of this work. However, before doing this, we review the main general properties that are believed to characterize the core of a neutron star.

2.1.3 The core

The core matter is characterized by densities $> 10^{14}\, g/cm^3$ and it can be thought as an homogeneous fluid of p, n, e^- in β equilibrium. At higher densities several processes may occur. For instance, as density increases electrons becomes more energetic and therefore their chemical potential, that is the energy needed to insert in a gas in equilibrium a new particle in the same state, increases too. As the electrons chemical potential exceeds the rest mass of the muon $m_\mu = 100\, MeV$ the neutron decay

$$n \to p + \mu^- + \bar{\nu}_\mu \tag{2.8}$$

becomes energetically more convenient than the β decay. Therefore we now have also some muons composing the core matter. At these densities the main contribute to pressure must comes from neutrons, however it cannot be associated only to Pauli exclusion principle because in this framework we can no longer consider the neutrons as non-interacting particles as we did for electrons in the white dwarfs. However, we just mentioned that the treatment of the interacting problem is made very complex by the very nature of the strong interactions. Thus the EOS of matter at these supernuclear densities depends on the particular model employed in the description of neutron interactions.

2.2 EOS models for neutron star matter

The description of matter at nuclear ($\sim \rho_0$) and supernuclear ($> \rho_0$) densities has to face many difficulties that are primarily related to the complexity of strong interactions and to the necessary approximations one have to make in order to describe many particles system. Every model proposed present unavoidably advantages and disadvantages. For instance the approach based on non-relativistic many body theory and phenomenological hamiltonian, even if succeeds in a good description of nuclear bound states and nucleon-nucleon scattering data, it doesn't fulfill the constraint of causality predicting a superluminal value for the speed of sound in matter at high density. On the other hand, an approach based on relativistic quantum fields theory while fulfilling the constraint of causality it provides an oversimplified dynamics, also affected by the uncertainty associated to the mean field approximation.

A pure phenomenological approach is also impossible because of the scarce empirical information. Indeed the study of matter at supernuclear densities is impossible in ordinary laboratory. However even if the experimental data are not sufficient to build up a satisfactionary model we can still use them to establish general constraints that every good theoretical model must satisfy.

In this section we will first summarize the empirical constraints we are able to impose on the EOS of cold matter, then we will outline the current understanding of the nucleon-nucleon (NN) interaction and finally we review the main features of the non relativistic and the relativistic approaches employed in the study of nuclear and supernuclear neutron star matter. In this last part we don't get too much into details, because of the complexity and the depth of the argument, but we will resume the most important logical steps one have to follow in order to construct such a model.

2.2.1 Nucleon-nucleon interaction

First of all we resume the main features of the nucleon-nucleon (NN) interaction that can be inferred by the empirical analysis.

The *saturation* of nuclear density i.e. the fact that the interior density of the atomic nuclei is independent by the mass number A for large A, as illustrated in fig. 2.2, tells us that nucleons cannot be put arbitrarily close to each other. Therefore, even if we know that NN force have to be in some sense attractive (otherwise we wouldn't have the formation of atomic nuclei), it must become strongly repulsive at short range. Therefore if we assume that the NN interaction can be write as a non relativistic potential v that depends on the interparticle distance $\vec{r}$, we have:

$$v(\vec{r}) > 0, \quad |\vec{r}| < r_c, \tag{2.9}$$

r_c being the radius of repulsive core.

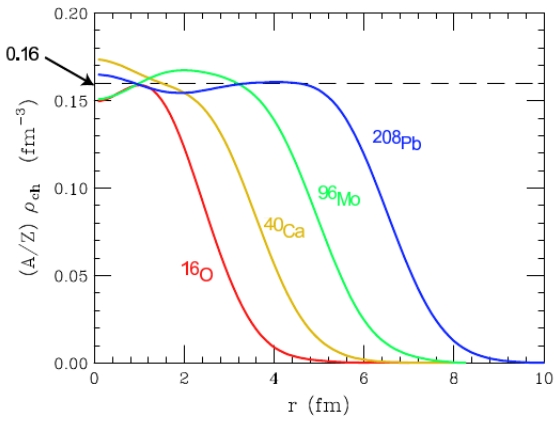

Figure 2.2. Saturation of central nuclear densities measured by electron-nucleus elastic scattering.

Another indication can be provided by the fact that the nuclear binding energy per nucleon is roughly the same for all nuclei with mass number $A \geq 20$. This suggest that the force present a finite interaction range, because after reaching a definite number of nucleons the introduction of a further one doesn't change the binding energy of a single nucleon, therefore the interaction must be not sensible to nucleons which are too much distant than a certain range. Thus we can write:

$$v(\vec{r}) = 0, \quad |\vec{r}| > r_0. \tag{2.10}$$

The spectra of the so called *mirror nuclei*, that exhibit striking similarities is another interesting point. Mirror nuclei are pairs of nuclei having the same A but an atomic number Z that differs by a unit from each other. The fact that the energy levels with same parity and angular momentum of such a nuclei are the same up to small electromagnetic corrections, tells us that neutron and proton have similar

nuclear interactions, i.e. that nuclear forces are charge symmetric. Charge symmetry is a manifestation of a more general invariance the *isospin symmetry*. It is well known that proton and neutron have nearly the same mass, this fact reflects the existence of a symmetry connecting proton and neutron that is only weakly broken by the existence of the electromagnetic interactions. If one assumes that proton and neutron are point particles [2] we can therefore write the lagrangian density:

$$\mathcal{L} = \bar{\psi}_i^N (i\gamma^\mu \partial_\mu - m)\psi_i^N + Interactions, \tag{2.11}$$

where the index i labels the type of nucleon (proton or neutron) and the Einstein convention is employed. We outline that ψ^N is an object with two components and each of them is a four components spinor:

$$\psi^N = \begin{pmatrix} \psi_p \\ \psi_n \end{pmatrix}, \tag{2.12}$$

with ψ_p and ψ_n labels respectively proton and neutron.

Let us concentrate on the kinetic part of (2.11); it is clearly invariant under the global $SU(2)$ transformation group defined by:

$$\psi_i^N \to \psi'^N_i = U_{ij}\psi_j^N \tag{2.13}$$

with:

$$U_{ij} = e^{ig^a T^a_{ij}}. \tag{2.14}$$

In equation (2.14) the g^a are continuous parameters ($a = 1, 2, 3$) and the T^a are the generators of the group, that in the special case of $SU(2)$ can be identified with the three Pauli matrices $(\sigma^1, \sigma^2, \sigma^3)$. The Pauli matrices are 2×2, hermitian and satisfying:

$$[\sigma^a, \sigma^b] = 2i\epsilon^{abc}\sigma^c. \tag{2.15}$$

Equation (2.12) shows that a nucleon can be described as a doublet in a spin-like space, named isospin space. Proton and neutron therefore represent the two isospin projections (related to $\sigma^3/2$), $+1/2$ and $-1/2$ respectively. Using the classical composition rules we can finally conclude that: proton-proton and neutron-neutron pairs always have total isospin $T = 1$, whereas a proton-neutron pair may have either $T = 0$ or $T = 1$. The two nucleon isospin states $|T, T_3\rangle$ can be summarized as follows:

$$\begin{aligned} |1,1\rangle &= |p,p\rangle \\ |1,0\rangle &= \tfrac{1}{\sqrt{2}}\left(|p,n\rangle + |n,p\rangle\right) \\ |1,-1\rangle &= |n,n\rangle \\ |0,0\rangle &= \tfrac{1}{\sqrt{2}}\left(|p,n\rangle - |n,p\rangle\right). \end{aligned} \tag{2.16}$$

Isospin invariance implies that the interaction between two nucleons depends on their total isospin T but not on T_3, because T_3 doesn't commute with a generic $SU(2)$ isospin transformation.

Other important details of the NN interaction are provided by the study of the two-nucleon system. In nature it is observed only one NN bound state: the nucleus

[2] This is clearly false, since they are bound states of three quarks, but it is not important if we are interest in energies not so high to resolve the internal structure of such particles.

of deuterium, or deuteron (^2H), composed by a proton and a neutron with total spin and isospin $S = 1$ and $T = 0$. This is a clear manifestation that nuclear forces are spin-isospin dependent. Another important information is that the deuteron exhibits a non-vanishing electric quadrupole moment, implying that its charge distribution is not spherically symmetric. Hence, the NN interaction in noncentral.

2.2.2 Phenomenological NN potential

Other important information, about the nature of the nuclear forces, are provided by the large data base coming from NN scattering experiments. In this paragraph we want to discuss a reasonable form of the potential that rules the NN interactions.

The first theoretical description of the interactions between two nucleons was attempted by Yukawa in 1935. He made the hypotesis that such a force was mediated by a particle corresponding to an energy qauntum of the nuclear field (in accordance to the well understood model of the electromagnetic interaction, according to which the photon is a quantum of the electromagnetic field). The fact that observations suggest that nuclear interactions have a finite range $r_0 \sim 1 \div 2\, fm$, combined with the indetermination relation $\Delta E \Delta t \sim 1$, leads Yukawa to estimate the mass m of the mediator to be:

$$m \sim \frac{1}{r_0} = \frac{1}{1 \div 2\, fm} = 100 \div 200\, MeV. \tag{2.17}$$

The idea of Yukawa was successfully implemented identifying the exchanged particle with the π-meson (*pion*) whose mass is $m_\pi \sim 139.6\, MeV$. Experiments shows that the pion is a spin zero pseudoscalar particle that comes in three charge states denoted π^+, π^-, and π^0. Let's see how to build a lagrangian that embodies the Yukawa's idea accounting in addition the observation that nuclear interactions conserve parity. We have to start by the kinetic therm of equation (2.11) and add an interaction term that fulfill all our requirements about the symmetry properties of the system. The most simple case is the interaction with a scalar boson Π, that leads to the lagrangian density:

$$\mathcal{L} = \bar{\psi}^N (i\gamma^\mu \partial_\mu - m)\psi^N + \mathcal{L}_\Pi + g\bar{\psi}^N \Pi \psi^N, \tag{2.18}$$

where we have suppressed the nucleonic indices, while $\mathcal{L}_\Pi$ contains the Π kinetic terms and its self interactions.

We know that nuclear interactions are charge symmetric therefore the total lagrangian must be $SU(2)$ invariant. This requirement leads to the transformation rule for the field Π:

$$\Pi \to \Pi' = U \Pi U^\dagger \tag{2.19}$$

that tells us that the field Π must be an object that lives in the adjoint representation of $SU(2)$. We can therefore write:

$$\Pi = \pi^a T^a \tag{2.20}$$

where T^a are the generators of $SU(2)$ in the fundamental representation. Since a runs from 1 to 3 we have found that the field mediating the interaction must be a triplet of isospin with components π^a. If π was a scalar, then according to the

renormalization criterion we would add to the lagrangian other terms, satisfying parity, such as Π or Π^3, which will complicate the Π self interactions. In order to eliminate all odd powers of Π, one could require Π to be a pseudoscalar and luckily this in what really happens in nature[3]. The interaction lagrangian now becomes:

$$\mathcal{L}_I = g\pi^a T^a_{ij} \bar{\psi}^N_i \gamma^5 \psi^N_j, \tag{2.21}$$

where we added γ^5 in order to conserve parity since we imposed that π is pseudoscalar. Armed with this lagrangian we can now study the nucleon-nucleon scattering at the leading order in perturbation theory. This process is described by the Feynman diagram in figure 2.3.

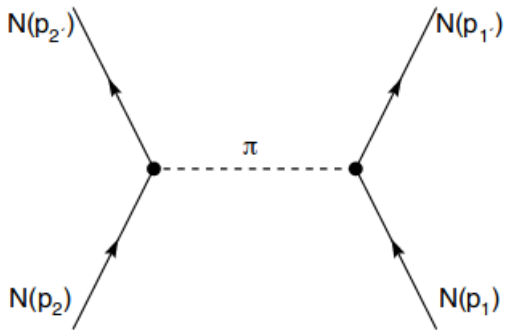

Figure 2.3. Feynman diagram describing the one pion exchange process between two nucleons. Time goes from bottom to top.

We have an initial state $|i\rangle = |p_1,\, s_1;\, p_2,\, s_2\rangle$, made by two nucleons with momentum p_1, p_2 and spin polarization s_1, s_2 respectively, which goes into a final state $|f\rangle = |p_{1'},\, s_{1'};\, p_{2'},\, s_{2'}\rangle$. Really we have to assign to each nucleon a further quantum number which labels if it is a proton or a neutron, i.e. its isospin projection.

From eq. (2.21) follows that we can take as interaction vertex the quantity $ig\gamma^5 T^a_{ij}$. We can now evaluate the invariant amplitude of the process using the standard Feynman's diagram techniques, obtaining:

$$i\mathcal{M} = -g^2\, \bar{u}(p_{2'}, s_{2'})\gamma^5 u(p_2, s_2) \frac{1}{k^2 - m_\pi^2} \bar{u}(p_{1'}, s_{1'})\gamma^5 u(p_1, s_1) \langle T^a_1 \rangle \langle T^a_2 \rangle, \tag{2.22}$$

where

$$\langle T^a_1 \rangle = \eta^\dagger_{1'} T^a \eta_1; \quad \langle T^a_2 \rangle = \eta^\dagger_{2'} T^a \eta_2 \tag{2.23}$$

with η_i being the two component Pauli spinor which defines the isospin state of the i-th nucleon.

In the non-relativistic limit (2.22) leads to define a NN interaction potential that

[3]Observing the process $\pi^- + d \to n + n$ it was established that the intrinsic parity of the pion is negative.

can be written in coordinate space as

$$\begin{aligned} v_\pi(\vec{r}) &= \frac{g^2}{4m^2} T_1^a T_2^a \left(\vec{\sigma_1}\cdot\vec{\nabla}\right)\left(\vec{\sigma_2}\cdot\vec{\nabla}\right)\frac{e^{-m_\pi r}}{r} = \\ &= \frac{g^2}{(4\pi)^2}\frac{m_\pi^3}{4m^2}\frac{1}{3}T_1^a T_2^a \left\{\left[(\vec{\sigma_1}\cdot\vec{\sigma_2}) + S_{12}\left(1+\frac{3}{x}+\frac{3}{x^2}\right)\right]\frac{e^{-x}}{x} + \right. \\ &\left. -\frac{4\pi}{m_{pi}^3}(\vec{\sigma_1}\cdot\vec{\sigma_2})\,\delta^{(3)}(\vec{r})\right\}, \end{aligned} \tag{2.24}$$

where $x = m_\pi r$, T_i^a is the generator of $SU(2)$ acting on the i-th particle and

$$S_{12} = \frac{3}{r^2}(\vec{\sigma_1}\cdot\vec{r})(\vec{\sigma_2}\cdot\vec{r}) - (\vec{\sigma_1}\cdot\vec{\sigma_2}), \tag{2.25}$$

is a reminiscent of the operator describing the noncentral interaction between two magnetic dipoles.

For $g^2/4\pi = 14$ the above potential provides an accurate description of the long range part ($r > 1.5\,fm$) of the NN interaction as shown by the very good fit of the NN scattering data with states of high angular momentum. In these states, due to the strong centrifugal barrier, the probability of finding the two nucleons at small relative distance is indeed negligible. At medium and short range other more complicated processes have to taken into account. In particular, when the relative distance becomes very small, $\sim 0.5\,fm$, nucleons, being composite objects of finite size, are expected to overlap. In this regime the interaction should be in principle dictated by quantum chromodynamics (QCD), the fundamental theory of strong interactions. In order to account of all these effects, for a good description of the full NN interaction it is necessary to employ a phenomenological potential, that usually can be written as

$$v = \tilde{v}_\pi + v_R, \tag{2.26}$$

where $\tilde{v}_\pi$ is the potential given by eq. (2.24) striped of the δ-function contribution and v_R describes the interactions at medium and short range. This potential can be conveniently rewritten in the form:

$$v = \sum_{S,T}\left[v_{TS}(r) + \delta_{S1}v_{tT}(r)S_{12}\right]P_S\Pi_T. \tag{2.27}$$

In the above equation S and T run over the possible total spin and isospin of the interacting pair, r is the distance between the two particles, S_{12} is given by (2.25) and P_S and Π_T are two projection operators. P_S ($S = 0,\,1$) are the spin projection operators defined through:

$$P_0 = \frac{1}{4}(1 - \vec{\sigma_1}\cdot\vec{\sigma_2})\ ,\ P_1 = \frac{1}{4}(3 + \vec{\sigma_1}\cdot\vec{\sigma_2}) \tag{2.28}$$

satisfying:

$$P_0 + P_1 = 1\ ,\ P_S|S'\rangle = \delta_{SS'}|S'\rangle\ ,\ P_S P_{S'} = \delta_{S'S}P_S, \tag{2.29}$$

in the last identity the Einstein convention is not employed. The projector Π_T is defined in the same way, but on the isospin space, therefore one have to make

the substitution $\sigma^a \to T^a$. The terms $v_{TS}(r)$ and $v_{tT}(r)$ are two coefficients that depend only on the relative distance between the interacting nucleons, therefore they account for the radial dependence of the interaction and have to approach to the corresponding components of the one pion exchange potential in the limit of large r. Their shapes are chosen to fit the available empirical data about the NN measurements. Since in general this potential is used to describe a many-body problem it is usually written expliciting the indices that label the particles that are involved. If we substitute the explicit form of the projectors into (2.27), we can write the potential ruling the interaction between the nucleons i and j as

$$v_{ij} = \sum_{n=1}^{6} v^{(n)}(r_{ij}) O_{ij}^{(n)}, \tag{2.30}$$

where

$$O_{ij}^{(n)} = 1,\ \left(T_i^a T_j^a\right),\ \left(\sigma_i^a \sigma_j^a\right),\ \left(T_i^a T_j^a\right)\left(\sigma_i^a \sigma_j^a\right),\ S_{ij},\ S_{ij}\left(\sigma_i^a \sigma_j^a\right); \tag{2.31}$$

and $v^{(n)}(r_{ij})$ are linear combinations of $v_{TS}(r)$ and $v_{tT}(r)$.

Finally we remark that can be shown that the operators $O_{ij}^{(n)}$ form an algebra as they satisfy:

$$O_{ij}^{(n)} O_{ij}^{(m)} = K_{nml}\, O_{ij}^{(l)}. \tag{2.32}$$

In figure 2.4 is illustrated the radial dependence $v(r_{ij})$ of the phenomenological potential in the case of zero relative angular momentum ($l = 0$), $S = 0$ and $T = 1$.

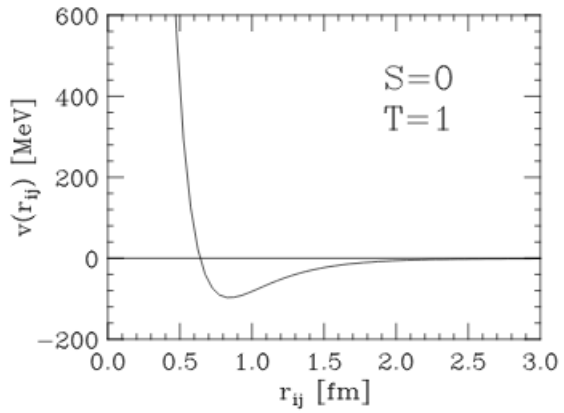

Figure 2.4. Radial dependence of the NN phenomenological potential that describes the interaction between two nucleons in the state characterized by relative angular momentum $l = 0$, and total spin and isospin respectively $S = 0$ and $T = 1$.

2.2.3 Non relativistic many-body theory

Nuclear matter can be thought of as a giant nucleus consisting of Z protons and $A - Z$ neutrons, in the limit of A, $Z \to \infty$, interacting through nuclear forces

only. Therefore we can try to understand the behavior of such a system within the non-relativistic many body theory (NMBT). In this framework we consider nucleons as point-like particles whose dynamics is governed by the Hamiltonian:

$$\mathcal{H} = \sum_i \frac{p_i^2}{2m} + \sum_{i<j} v_{ij} + \sum_{i<j<k} V_{ijk}. \tag{2.33}$$

In the above equation p_i is the momentum of the i-th particle, v_{ij} is the potential that accounts for the NN interactions and V_{ijk} is the potential related to processes involving three nucleons. This last must be introduced in order to explain the properties of nuclei with $A = 3$, for which the Schrödinger equation:

$$\mathcal{H}|\Psi_0\rangle = E_0|\Psi_0\rangle \tag{2.34}$$

can still be solved exactly. We can imagine the potential V_{ijk} of the form:

$$V_{ijk} = V_{ijk}^{2\pi} + V_{ijk}^{N}\,, \tag{2.35}$$

where the first term accounts for the two-pions exchange process, while the second one is purely phenomenological. About the form of v_{ij} one can take the expression given in the previous paragraph, but there also exist improved versions of it that take into account a greater number of operators [5].

As already said the equation (2.34) can be solved exactly only for $A \leq 3$, for greater A it is necessary to employ some approximations. However exist some calculation techniques that allow very good calculations for nuclei having A up to 8. Clearly in the neutron star core framework, where we have $A \sim 10^{57}$ the situation becomes very difficult. Let us first consider symmetric nuclear matter, defined as a uniform extended system containing equal numbers of protons and neutrons. Neglecting three-nucleon forces the overall hamiltonian can be written as in equation (2.33) stripped by the last term (V_{ijk}). In absence of interactions the wave function of such a system will be a Slater determinant of the single particle states:

$$\phi_{\vec{k}st}(\vec{r}) = \frac{1}{\sqrt{V}} e^{i\vec{k}\cdot\vec{r}} \chi_s \eta_t\,, \tag{2.36}$$

where χ and η are Pauli spinors describing spin and isospin respectively, and $k < k_F = (6\pi^2 n/\nu)^{1/3}$, with n and ν being respectively the particle density and the degeneracy of the momentum eigenstates. Once we have a complete set of energy eigenstates related to the non-interacting problem, it is naturally to try a perturbative approach, that unfortunately collides immediately with the very nature of the potential v_{ij}. As we can see from figure 2.4, due to the strong repulsive core, the matrix element of v_{ij} between two eigenstates of the "unperturbed" hamiltonian is very large or even divergent. This difficulty can be circumvented either through a redefinition of the interaction potential or changing the basis of states describing the "unperturbed" system. The first approach, that leads to the technique of the G-matrix perturbation theory, that is reviewed in [4] will be left apart in this work. We will concentrate on the approach of the so called Correlated Basis Functions (CBF) effective interaction, since one of the EOSs employed for the tidal Love number calculation, made in this work, is obtained in this framework.

2.2.4 CBF effective interaction

The formalism of correlated basis functions is based on the variational approach to the many body problem. The variational approach is based on the variational principle of quantum mechanics. Let us consider a general eigenvalues problem:

$$\mathcal{H}|E_i\rangle = E_i|E_i\rangle. \tag{2.37}$$

The set of eigenstates $|E_i\rangle$ of $\mathcal{H}$ forms a basis of the Hilbert space of the system, we can therefore write a generic state $|\alpha\rangle$ as

$$|\alpha\rangle = \sum_i C_i^{(\alpha)}|E_i\rangle. \tag{2.38}$$

If we take the expectation value of $\mathcal{H}$ on $|\alpha\rangle$, we have

$$\langle\alpha|\mathcal{H}|\alpha\rangle = \sum_i |C_i^{(\alpha)}|^2 E_i \geq E_0\langle\alpha|\alpha\rangle. \tag{2.39}$$

The above equation implies that as the quantity

$$\frac{\langle\alpha|\mathcal{H}|\alpha\rangle}{\langle\alpha|\alpha\rangle} \tag{2.40}$$

approaches its minimum, $|\alpha\rangle$ approaches $|E_0\rangle$. We can therefore search for a good approximation of the ground state by minimizing the expectation value of the total hamiltonian on a trial state. For a better choice of the trial state the approximation will be better. Within this scheme, the trial ground state is chosen of the form:

$$|\Psi_0\rangle = \frac{\mathcal{F}|\Phi_0\rangle}{\langle\Phi_0|\mathcal{F}^\dagger\mathcal{F}|\Phi_o\rangle^{1/2}}\,, \tag{2.41}$$

where the ket $|\Phi_0\rangle$ is the ground state of the non-interacting hamiltonian, and $\mathcal{F}$ is an operator that embodies the effects of correlation among the nucleons. The structure of $\mathcal{F}$ is chosen to mirror the structure the NN interaction potential, thus we have

$$\mathcal{F} = \mathcal{S}\prod_{i<j} F_{ij} \tag{2.42}$$

with

$$F_{ij} = \sum_{p=1}^{N} f^p(r_{ij})O_{ij}^p\,, \tag{2.43}$$

where $\mathcal{S}$ is the symmetrization operator that is needed to fulfill the requirement of antisymmetry for $|\Psi_0\rangle$ ($|\Phi_0\rangle$ is antysimmetric), and N is the number of operators used to build the potential v_{ij} (in the case we exposed before is $N = 6$). The coefficients $f^p(r_{ij})$ that describe the radial dependence of the correlation functions are determined by functional minimization of the quantity:

$$E_V = \langle\Psi_0|\mathcal{H}|\Psi_0\rangle. \tag{2.44}$$

This procedure leads to a set of Euler-Lagrange equations whose solutions satisfy the boundary conditions:

$$\lim_{r\to\infty} f^p(r) = \begin{cases} 1 & p = 1 \\ 0 & p > 1 \end{cases} \tag{2.45}$$

that implies that for large interparticle distances the correlation effect becomes negligible and the state approaches the one of the non-interacting problem. The calculation of the variational energy of eq. (2.44) involves severe difficulties, that can be overcome using specific calculation techniques such as cluster expansion or variational Monte Carlo methods, that will be not treated in this work.

Under the assumption that the correlation structure of the ground and excited states is the same, the operator $\mathcal{F}$, obtained from the variational calculation of E_V, can be used to generate a complete, nonorthogonal set of correlated excited states though the replacement $|\Phi_0\rangle \to |\Phi_n\rangle$.

Once the correlated basis has been defined we can split the nuclear hamiltonian in two pieces

$$\mathcal{H} = H_0 + H_1 \tag{2.46}$$

where H_0 and H_1 are defined as the diagonal and off-diagonal part of $\mathcal{H}$ between two correlated states according to:

$$\langle\Psi_m|H_0|\Psi_n\rangle = \delta_{mn}\langle\Psi_m|\mathcal{H}|\Psi_n\rangle \tag{2.47}$$

$$\langle\Psi_m|H_1|\Psi_n\rangle = (1-\delta_{mn})\langle\Psi_m|\mathcal{H}|\Psi_n\rangle. \tag{2.48}$$

If we made a good choice for the correlation function, i.e. if the value of E_V is close to the real value of the ground state energy of the system E_0, then states $|\psi_n\rangle$ have a great overlap with the real eigenstates of the nuclear hamiltonian $\mathcal{H}$, therefore the braket of H_1 between these states will be small and H_1 could be treated in perturbation theory.

In the approach we developed above, one have to evaluate the matrix elements of $\mathcal{H}$ between the new set of states; however the same results can be obtained transforming the hamiltonian and using the Fermi gas basis. This procedure leads to the appearance of an effective hamiltonian suitable for perturbative calculations, avoiding the nontrivial difficulties arising from the use of a nonorthogonal basis.

We can therefore define a CBF effective interaction through the matrix elements of the nuclear hamiltonian in the correlated ground states, as

$$\langle\Psi_0|\mathcal{H}|\Psi_0\rangle = T_F + \langle\Phi_0|\sum_{i<j} v_{ij}^{\text{eff}}|\Phi_0\rangle \tag{2.49}$$

where T_F is the energy of the free Fermi gas, and the effective potential is written in the same form of v_{ij}:

$$v_{ij}^{\text{eff}} = \sum_p v^{\text{eff},\,p}(r_{ij})O_{ij}^p. \tag{2.50}$$

The potential v_{ij}^{eff} now embodies the effect of correlations and therefore it is expected to have a good behavior for short and long distances. As a proof we report, in Fig. 2.5 (taken from [5]), the plot of the radial dependence of the spherically symmetric

component of the potential between two nucleons, coupled with total spin and isospin $S = 1$, $T = 0$, as it appears both in the bare potential v_{ij} (dashed line) and in the CBF effective interaction (solid line), calculated at $\rho = \rho_0$. From figure 2.5 it is clear that we achieved to remove the problem of the strong repulsive core that forbade a perturbative treatment.

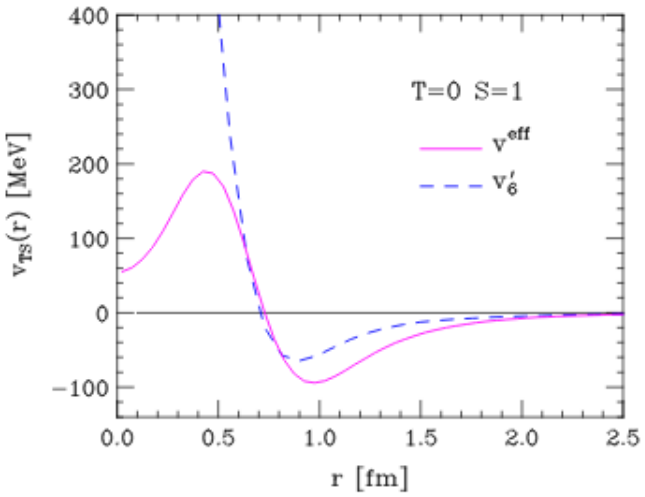

Figure 2.5. Radial dependence of the spherically-symmetric component of the bare potential (dashed line) and the CBF effective interaction (solid line) in the spin-isospin channel corresponding to $S = 1$ and $T = 0$. The effective interaction has been computed setting $\rho = \rho_0$.

2.2.5 Relativistic mean field theory: the $\sigma - \omega$ model

To conclude this chapter i quickly review the relativistic mean field approach, taking as example the $\sigma - \omega$ model. This model consist in an effective theory in which nuclear matter is viewed as a uniform system of nucleons, described by Dirac spinors, interacting through exchange of a scalar and a vector meson, called σ and ω, respectively. We can write the lagrangian of this theory as:

$$\mathcal{L} = \mathcal{L}_N + \mathcal{L}_B + \mathcal{L}_{\text{int}}, \tag{2.51}$$

where $\mathcal{L}_N$ and $\mathcal{L}_B$ are the free lagrangians of respectively the nucleons and the bosons. defined through:

$$\mathcal{L}_N = \bar{\psi}(x)\left(i\gamma^\mu \partial_\mu - m\right)\psi(x) \tag{2.52}$$

$$\begin{aligned} \mathcal{L}_B &= \mathcal{L}_\omega + \mathcal{L}_\sigma = \\ &= -\frac{1}{4}F^{\mu\nu}F_{\mu\nu} + \frac{1}{2}m_\omega^2 V_\mu(x)V^\mu(x) + \\ &+ \frac{1}{2}\partial_\mu\phi(x)\partial^\mu\phi(x) - \frac{1}{2}m_\sigma^2\phi^2(x)\,, \end{aligned} \tag{2.53}$$

with

$$F_{\mu\nu} = \partial_{nu}V_\mu(x) - \partial_\mu V_\nu(x). \tag{2.54}$$

In specifying the form of the interaction lagrangian we will require that, besides being a Lorentz scalar, $\mathcal{L}_{\rm int}$ gives rise to a Yukawa-like meson exchange potential in the static limit. Hence, we write

$$\mathcal{L}_{\rm int} = g_\sigma \phi(x)\bar{\psi}(x)\psi(x) - g_\omega V_\mu(x)\bar{\psi}(x)\gamma^\mu\psi(x), \tag{2.55}$$

where g_ω and g_σ are coupling constants.

From the variational principle we can derive the Euler-Lagrange equations of motion for this system that are:

$$\begin{aligned}
&(\Box + m_\sigma^2)\phi(x) = g_\sigma\bar{\psi}(x)\psi(x);\\
&(\Box + m_\omega^2)V_\mu(x) - \partial_\mu(\partial^\nu V_\nu(x)) = g_\omega V_\mu(x)\bar{\psi}(x)\gamma^\mu\psi(x);\\
&\left[(\gamma^\mu\partial_\mu - g_\omega\gamma^\mu V_\mu(x)) - (m - g_\sigma\phi(x))\right]\psi(x) = 0.
\end{aligned} \tag{2.56}$$

The above equations present insurmountable calculation difficulties that cannot be circumvented using approximations based on perturbation theory, therefore here we have to use a different scheme: the *mean field approximation*. This approximation amounts to treat $V_\mu(x)$ and $\phi(x)$ as classical fields, replacing in the equations of motion their mean values in the ground state of uniform nuclear matter

$$\phi(x) \to \langle\phi(x)\rangle\,, \quad V_\mu(x) \to \langle V_\mu(x)\rangle. \tag{2.57}$$

Keeping in mind that in uniform nuclear matter the baryon and scalar densities, $n_B = \langle\psi^\dagger\psi\rangle$ and $n_s = \langle\bar{\psi}\psi\rangle$, as well as the current $j^\mu = \langle\bar{\psi}\gamma^\mu\psi\rangle$ are constants independent of x, the quantities $\langle\phi(x)\rangle$ and $\langle V_\mu(x)\rangle$ can be easily calculated from the equations of motion. Finally we obtain the Euler-Lagrange equation for $\psi(x)$ to be:

$$\left[(\gamma^\mu\partial_\mu - g_\omega\gamma^\mu\langle V_\mu\rangle) - (m - g_\sigma\langle\phi\rangle)\right]\psi(x) = 0, \tag{2.58}$$

that can be solved for a ψ of the form

$$\psi(x) = \psi_{\vec{k}}\, e^{ikx}. \tag{2.59}$$

For brevity we now skip the details and limit ourselves to observe that in order to obtain the equation of state, i.e. the relation between pressure and matter density (or energy density), we can use the fact that in a uniform system the expectation value of the energy-momentum tensor $T^{\mu\nu}$ is directly related to energy density and pressure thorough

$$\langle T^{\mu\nu}\rangle = u_\mu u_\nu\,(\epsilon + P) - g_{\mu\nu}P \tag{2.60}$$

where u is the four velocity of the system satisfying $u_\mu u^\mu = 1$, and $T^{\mu\nu}$, for a generic $\mathcal{L} = \mathcal{L}(\phi, \partial_\mu\phi)$ is defined as

$$T^{\mu\nu} = \frac{\partial\mathcal{L}}{\partial(\partial_\mu\phi)}\partial^\nu\phi - g^{\mu\nu}\mathcal{L}. \tag{2.61}$$

Chapter 3

Stellar structure models for neutron stars

In the previous chapter we fully analyze the main features and problems concerning the internal structure of the neutron stars. Our ultimate goal was to define a consistent model that describes the equation of state of such an object. However, in order to extract some useful predictions we have to relate the properties concerning the EOS to observable astrophysical quantities. In the case of white dwarfs we have seen that such a relation is provided by the stellar structure equations, therefore one is tempted to employ the same reasoning in the case of neutron stars. Unfortunately there still is complication. For white dwarf we had that their typical mass and radius satisfy: $GM/Rc^2 \sim 10^{-4}$, whereas for neutron stars we have: $GM/Rc^2 \sim 10^{-1}$. In this last case the condition $GM/Rc^2 << 1$ is not fulfilled and we can no longer neglect the effect of space-time curvature, therefore in order to describe the gravitational behavior of such compact stars we must use the Einstein theory of General Relativity instead of the classical newtonian gravity.

3.1 General Relativity

General Relativity is the spacetime theory of gravity proposed by Einstein in 1915, that attributes the nature of the gravitational phenomena to the curvature of the space-time that is viewed for the first time as an active physical entity instead of a mere background in which physical events happen. General Relativity is entirely base on two principles:

- the Equivalence Principle, stating that at any given spacetime point is always possible to chose a local inertial reference frame surrounding that point, in which the physical laws are the same that act in absence of gravity i.e. the ones described by special relativity;
- the Principle of General Covariance stating that physical laws must have the same form in every coordinate system i.e. they must be generally covariant.

Let's spend two words on the Equivalence Principle and see why it implies that gravity could be related to space-time curvature. Before that Einstien published his

work, Gauss identified a class of metric spaces in which the curvature could locally be ruled out. The concept of curvature is strongly related to the concept of distance between two points. Stating that the curvature can be locally deleted is equivalent to say that the distance between two points, that are sufficiently close to each other, can be computed using the usual euclidean formula:

$$ds^2 = \sum_{i=1}^{N} dx_i^2, \tag{3.1}$$

where N is the dimension of the metric space. For example if take as a metric the space the surface of a sphere, we are assuming that there always exist two points that are close enough such that the distance between them is given by the theorem of Pitagora. Let's come back to the Equivalence principle: saying that locally the physical laws assume the form given by special relativity implies that the distance between two points is given by

$$ds^2 = -dx_0^2 + \sum_{i=1}^{3} dx_i^2. \tag{3.2}$$

Therefore the equivalence principle resembles very much the axiom that Gauss chose as the basis for the non-euclidean geometries. We therefore expect that, according to this principle, the equations of gravity will look very similar to those of Riemannian geometry. The meaningful quantity in such a framework becomes the metric tensor $g_{\mu\nu}$, that allows us to compute the distance between two points, according to

$$ds^2 = g_{\mu\nu} dx^\mu dx^\nu. \tag{3.3}$$

The metric tensor depends on the space-time point in which is evaluated, it is $g_{\mu\nu} \equiv g_{\mu\nu}(x)$, and therefore on the particular choice of coordinate that is made. In a locally inertial frame (LIF) we have $g_{\mu\nu} = \eta_{\mu\nu}$ with

$$\eta_{\mu\nu} = \begin{pmatrix} -1 & 0 & 0 & 0 \\ 0 & 1 & 0 & 0 \\ 0 & 0 & 1 & 0 \\ 0 & 0 & 0 & 1 \end{pmatrix}. \tag{3.4}$$

Being ξ^α a set of coordinates in a LIF and x^α a coordinate set in a generic reference frame we have

$$ds^2 = \eta_{\mu\nu} d\xi^\mu d\xi^\nu = \eta_{\mu\nu} \frac{\partial \xi^\mu}{\partial x^\alpha} \frac{\partial \xi^\mu}{\partial x^\beta} dx^\beta dx^\alpha = g_{\alpha\beta} dx^\alpha dx^\beta. \tag{3.5}$$

From the last equation we point out the transformation law for the metric tensor (and for a rank 2 tensor in general):

$$\begin{aligned} x^\alpha &\to x^{\alpha'}(x^\mu) \\ g_{\alpha\beta} &\to g_{\alpha'\beta'} = \frac{\partial x^\mu}{\partial x^{\alpha'}} \frac{\partial x^\nu}{\partial x^{\beta'}} g_{\mu\nu} \equiv \Lambda^\mu_{\alpha'} \Lambda^\nu_{\beta'}\, g_{\mu\nu}. \end{aligned} \tag{3.6}$$

We define the inverse metric $g^{\mu\nu}$ as:

$$g^{\mu\alpha} g_{\alpha\nu} = \delta^\mu{}_\nu, \tag{3.7}$$

that allow us to raise and lower a tensor index through

$$A^{\mu}{}_{\nu} = g^{\mu\alpha} A_{\alpha\nu}. \tag{3.8}$$

We can deduce also the geodesic equation, i.e. the equation of motion of a particle under the effect of the gravity only when observed in a generic reference frame. If ξ^{α} are the coordinates in a LIF and τ is the proper time of the particle we have:

$$\frac{d^2\xi^{\alpha}}{d\tau^2} = 0. \tag{3.9}$$

Using the general coordinate transformation $\xi^{\alpha} = \xi^{\alpha}(x^{\mu})$ and after making some composite derivative we get:

$$\frac{d^2x^{\alpha}}{d\tau^2} + \Gamma^{\alpha}_{\mu\nu}\left[\frac{dx^{\mu}}{d\tau}\frac{dx^{\nu}}{d\tau}\right] = 0, \tag{3.10}$$

where the quantities

$$\Gamma^{\alpha}_{\mu\nu} = \frac{\partial x^{\alpha}}{\partial \xi^{\lambda}} \frac{\partial \xi^{\lambda}}{\partial x^{\mu} \partial x^{\nu}} \tag{3.11}$$

are named *affine connections* or *Christoffel symbols* and satisfies also:

$$\Gamma^{\alpha}_{\mu\nu} = \frac{1}{2}\, g^{\alpha\lambda}\left(g_{\mu\lambda,\nu} + g_{\lambda\nu,\mu} - g_{\mu\nu,\lambda}\right). \tag{3.12}$$

We remark the fact that the affine connections aren't tensors since they don't obey the usual transformation rules. The Christoffel symbols can be used to define a *covariant derivative*, i.e. a derivative that when applied to a generic tensorial object provides that the resulting quantity still transforms like a tensor under a general coordinates transformation. If it is applied to a 4-vector it is defined as

$$V^{\mu}_{;\alpha} = V^{\mu}_{,\alpha} + \Gamma^{\mu}_{\alpha\beta} V^{\beta}. \tag{3.13}$$

It can be shown that $V^{\mu}_{;\alpha}$ transforms as a rank (1,1) tensor and that in a locally inertial frame it reduces to $V^{\mu}_{;\alpha} = V^{\mu}_{,\alpha}$.

All these considerations can be made more formals in the framework of the differentiable manifolds, but we won't go into details.

We limit ourselves to report the Einstein equations that embody the dynamics of the gravitation:

$$G_{\mu\nu} = \frac{8\pi G}{c^4} T_{\mu\nu}. \tag{3.14}$$

In the above equation $T^{\mu\nu}$ is the stress-energy tensor whose components are defined as follows. T_{00} is the energy density, T_{0i} is the energy which flows per unit time across a unit surface orthogonal to the axis x^i, and T_{ij} is the amount of the i-th component of momentum which flows per unit time across the unit surface orthogonal to the axis x^j. $G_{\mu\nu}$ is the so called Einstein tensor and is defined as

$$G_{\mu\nu} = \left(R_{\mu\nu} - \frac{1}{2} g_{\mu\nu} R\right), \tag{3.15}$$

where $R_{\mu\nu}$ and R are two quantities (that depend on the metric tensor and its first and second derivatives) that are related to the intrinsic curvature of the space-time. Equation (3.14) therefore connects the curvature of the space-time to the amount of mass-energy that is present in that spacetime point.

It is interesting to see in which limit the gravitational theory of Newton is restored. Let us consider a non relativistic particle in a weak and stationary gravitational field. Since $v << c$ it follows

$$\frac{dx^i}{dt} << c \;\; \Rightarrow \frac{dx^i}{d\tau} << \frac{cdt}{d\tau} = \frac{dx^0}{d\tau}. \tag{3.16}$$

The geodesic equation (3.10) therefore becomes

$$\frac{d^2x^\mu}{d\tau^2} + \Gamma^\mu_{00}\left(\frac{dx^0}{d\tau}\right)^2 = 0. \tag{3.17}$$

If we use the assumption that the field is stationary, i.e. we can take a time-independent metric tensor, according to equation (3.12) we have:

$$\Gamma^\mu_{00} = \frac{1}{2}g^{\mu\lambda}(g_{0\lambda,0} + g_{\lambda 0,0} - g_{00,\lambda}) = -\frac{1}{2}g^{\mu\lambda}g_{00,\lambda}. \tag{3.18}$$

The weak field limit can be interpreted as that we can chose a reference frame in which the metric is nearly flat, therefore:

$$g_{\mu\nu} = \eta_{\mu\nu} + h_{\mu\nu}, \qquad |h_{\mu\nu}| << 1. \tag{3.19}$$

Since we are interest in first order terms in $h_{\mu\nu}$ we can raise and lower its indices with the flat metrics $\eta_{\mu\nu}$. Substituting the form of the metrics into (3.18) we have

$$\Gamma^\mu_{00} \sim -\frac{1}{2}\eta^{\mu\lambda}\frac{\partial h_{00}}{\partial x^\lambda} \tag{3.20}$$

that put in (3.17) leads to:

$$\frac{d^2x^i}{d\tau^2} = \frac{1}{2}\frac{\partial h_{00}}{\partial x^i}\left(\frac{cdt}{d\tau}\right)^2. \tag{3.21}$$

If we rescale the time coordinate according to $cdt/d\tau = 1$ we find

$$\frac{d^2\vec{x}}{dt^2} = \frac{c^2}{2}\vec{\nabla}h_{00}, \tag{3.22}$$

and remembering that the corresponding newtonian equation is

$$\frac{d^2\vec{x}}{dt^2} = \vec{\nabla}\Phi, \tag{3.23}$$

if we take $\Phi = -GM/r$ and impose that h_{00} vanishes at infinity we finally have the correspondence we were looking for:

$$h_{00} = -2\frac{\Phi}{c^2} \quad \text{and} \quad g_{00} = -(1 + 2\frac{\Phi}{c^2}). \tag{3.24}$$

We finally outline the connection with the Einstein equations. It is known that Φ satisfies the Laplace equation, thus substituting (3.24) into the Laplace equation we find

$$\nabla^2 g_{00} = -\frac{8\pi G}{c^4}T_{00} \tag{3.25}$$

that is the limit in the case of weak stationary field for the $(0,0)$ component of the Einstein equations.

3.2 Relativistic stellar structure

3.2.1 The Tolman Oppenheimer and Volkoff equations

As we pointed out in the first part of the previous section, we are interest in writing the stellar structure equations in the framework of General Relativity. To this purpose we have to solve the Einstein equations in matter. First of all we want to point out the form that assumes the tensor $T^{\mu\nu}$ in the star interior. To hereafter we shall use geometric units $G = c = 1$.

As already said we can model a star as spherically symmetric, stationary perfect fluid in chemical, hydrostatic and thermodynamic equilibrium. A fluid is said perfect if both viscosity and heat flow are absent. The motion of the fluid is described by the vector field of the four-velocity u^α that will define a worldtube in the space-time. Now consider a small volume of the fluid and a point P_0 in its center of mass. We put ourselves in a reference frame that has P_0 as origin and that is locally inertial and such P_0 is at rest, we name it as a locally inertial comoving frame (LICF). We have to take into account a small worldvolume that must be small enough to be covered by the LICF and large enough with respect to the scale of the microscopic dynamics of the system. The fluid element enclosed in this worldvolume can be described by the usual thermodynamical quantities.

In this LICF the stress-energy tensor of the fluid assumes the following form:

$$T^{\mu\nu} = \begin{pmatrix} \epsilon & 0 & 0 & 0 \\ 0 & P & 0 & 0 \\ 0 & 0 & P & 0 \\ 0 & 0 & 0 & P \end{pmatrix} \tag{3.26}$$

where ϵ is the energy density and P is the pressure. The components T^{0i} vanish because the fluid is at rest and since there is no heat flux, the energy can't flow in any direction. The absence of viscosity instead put to zero the components T^{ij} with $i \neq j$.

Since we are in a LICF we also have:

$$g_{\mu\nu} = \eta_{\mu\nu} \quad \text{and} \quad u^\alpha = (1,\ 0,\ 0,\ 0)\,, \tag{3.27}$$

therefore $T^{\mu\nu}$ can be written as

$$T^{\mu\nu} = u^\mu u^\nu \left(\epsilon + P\right) + g_{\mu\nu} P, \tag{3.28}$$

that is a tensorial equation and therefore, for the principle of general covariance, it must be true in any other reference frame.

We can now look at Einstein equations that can be solved in addition with the condition imposing the energy and momentum conservation, i.e.

$$T^{\mu\nu}{}_{;\nu} = 0. \tag{3.29}$$

Since we are interest in the structure of a spherically symmetric, non rotating and stationary star, the most general metric according to these properties can be written as

$$ds^2 = g_{\mu\nu} dx^\mu dx^\nu = -e^{2\nu(r)} dt^2 + e^{2\lambda(r)} dr^2 + r^2 \left(d\theta^2 + \sin^2\theta\, d\phi^2\right), \tag{3.30}$$

thus

$$g_{\mu\nu} = \begin{pmatrix} -e^{2\nu(r)} & 0 & 0 & 0 \\ 0 & e^{2\lambda(r)} & 0 & 0 \\ 0 & 0 & r^2 & 0 \\ 0 & 0 & 0 & r^2 \sin^2\theta \end{pmatrix}. \tag{3.31}$$

With this metric and with the hypothesis that the fluid is at rest, the 4-velocity u^α is given by:

$$-1 = u^\alpha u^\beta g_{\alpha\beta} = (u^0)^2 g_{00} \Rightarrow u^\alpha = \left(e^{-\nu(r)},\ 0,\ 0,\ 0\right). \tag{3.32}$$

Remembering that $R_{\mu\nu}$ and R are defined respectively as

$$R_{\mu\nu} = \left(\Gamma^\alpha_{\mu\alpha,\nu} - \Gamma^\alpha_{\mu\nu,\alpha} - \Gamma^\alpha_{\mu\nu}\Gamma^\beta_{\alpha\beta} + \Gamma^\alpha_{\mu\beta}\Gamma^\beta_{\nu\alpha}\right) \tag{3.33}$$

and

$$R = g^{\mu\nu} R_{\mu\nu} \tag{3.34}$$

we can finally write the non vanishing components of the Einstein equations that give rise to:

$$\begin{aligned} &a) \quad G_{00} = 8\pi T_{00} \Rightarrow \frac{1}{r^2} e^{2\nu} \frac{d}{dr}\left[r\left(1 - e^{-2\lambda}\right)\right] = 8\pi\epsilon e^{2\nu} \\ &b) \quad G_{rr} = 8\pi T_{rr} \Rightarrow -\frac{1}{r^2} e^{2\lambda}\left(1 - e^{-2\lambda}\right) + \frac{2}{r}\nu_{,r} = 8\pi P e^{2\lambda} \\ &c) \quad G_{\theta\theta} = 8\pi T_{\theta\theta} \Rightarrow r^2 e^{-2\lambda}\left[\nu_{,rr} + \nu_{,r}^2 + \frac{\nu_{,r}}{r} - \nu_{,r}\lambda_{,r} - \frac{\lambda_{,r}}{r}\right] = 8\pi r^2 P. \end{aligned} \tag{3.35}$$

From equation (3.29) it follows

$$\nu_{,r} = -\frac{P_{,r}}{\epsilon + P}, \tag{3.36}$$

that combined with (3.35) leads to the final set of equations:

$$\begin{cases} \dfrac{dM(r)}{dr} = 4\pi r^2 \epsilon(r) \\ \dfrac{dP}{dr} = -\dfrac{\left[\epsilon(r) + P(r)\right]\left[M(r) + 4\pi r^3 P(r)\right]}{r\left[r - 2M(r)\right]} \end{cases} \tag{3.37}$$

where $M(r)$ is defined as:

$$M(r) = \frac{1}{2} r\left(1 - e^{-2\lambda(r)}\right). \tag{3.38}$$

The set of equations (3.37) are the so called Tolman, Oppenheimer and Volkoff (TOV) equations. The second equation of (3.37) can be rewritten as:

$$\frac{dP}{dr} = -\epsilon(r)\frac{GM(r)}{r^2}\left[1 + \frac{P(r)}{\epsilon(r)}\right]\left[1 + \frac{4\pi r^3 P(r)}{M(r)}\right]\left[1 - \frac{2GM(r)}{r}\right]^{-1}, \tag{3.39}$$

where we restored the gravitational constant G. We can now look at each term in this equation. The first term is the same that is present in its newtonian counterpart,

with the mass density replaced by the energy density. The second and third terms represent relativistic corrections that vanish when $P/\epsilon << 1$ i.e. when the constituents of matter are non-relativistic particles. Finally the last term accounts for spacetime curvature, indeed it vanishes when $GM/r << 1$. Therefore it is clear that in the non-relativistic limit the TOV equations reduce to the usual newtonian equations. Moreover we remark the fact that, equivalently to the non-relativistic case, these equations cannot be solved without the knowledge of the equation of state, i.e. the law $P(\epsilon)$, that describes the matter that made up the star.

3.2.2 Boundary conditions

The set of equations (3.37) in addition with a given EOS, $P(\epsilon)$, is a system of first order differential equations, therefore in order to be solved it requires three boundary conditions: $M(r_0)$, $P(r_0)$ and $\epsilon(r_0)$. Actually, since $P \equiv P(\epsilon)$ we need only two boundary conditions.

We can always chose as a boundary condition: $M(r = 0) = 0$. This choice is justified as follows. Take a tiny sphere of radius x, then the circumference is $2\pi x$ and the proper radius will be

$$\int_0^x e^{\lambda} dr \simeq e^{\lambda} x, \tag{3.40}$$

hence their ratio is $2\pi e^{-\lambda}$. However we know that the spacetime is locally flat and a flat spacetime implies that the ratio between the circumference and the radius of a sphere is 2π, therefore as $r \to 0$ then $e^{\lambda} \to 1$. Since holds the relation

$$e^{2\lambda} = \frac{1}{1 - \frac{2M(r)}{r}}, \tag{3.41}$$

it follows that $M(r)$ must tend to zero faster than r. We remark that the quantity

$$M(R) = 4\pi \int_0^R r^2 \epsilon(r) dr, \tag{3.42}$$

that has the same form as in the newtonian theory, can be interpreted as the total mass-energy inside the radius R.

For any assigned EOS now we have a one-parameter family of solutions, identified by the value of the energy density at $r = 0$, i.e. $\epsilon(r = 0) = \epsilon_0$. Outside the star, instead, $P = 0$ and $\epsilon = 0$, and the Einstein equations reduce to those in the vacuum, whose unique solution is given by the Schwarzschild metrics.

3.2.3 A necessary condition for the stability of a star

The solution of TOV equations with the appropriate boundary conditions, describes the equilibrium configuration of a star. In principle this equilibrium could be stable or unstable. We are now interest into discuss when one of these two possible scenarios may occur. Suppose to have solved the TOV equations for any value of the central energy density ϵ_0, i.e. to have found the function $M(\epsilon_0)$ that relates the total gravitational mass of the star to its central energy density.

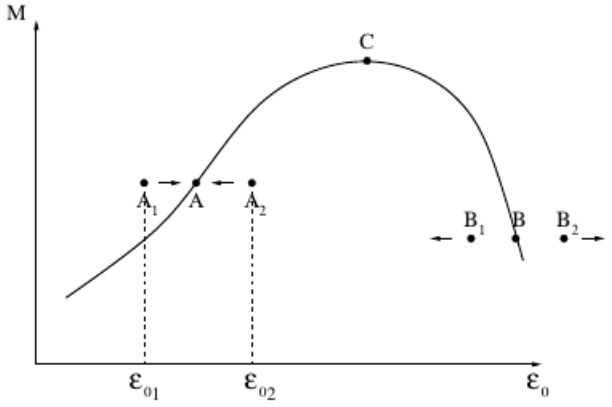

Figure 3.1. The mass of equilibrium stellar configurations as function of the central energy density.

A typical scenario that one faces is illustrated in the figure 3.1.

Now consider the equilibrium configuration, such that the one in the figure labeled by A. Let's consider a small perturbation of the central density, we can assist at two possible scenarios. If the density decreases to a value ϵ_{01} then the star has a mass that is above the value necessary to reach an equilibrium configuration (A_1 in the picture), therefore the gravitational attraction provides a further contraction that increases the density until its equilibrium value is reached. Conversely, if the density increases to a value ϵ_{02}, therefore the star is in a configuration (A_2) in which its mass is below the value required for hydrostatic equilibrium, therefore the pressure exceeds gravity and provides a further expansion that raises up the density and brings the star again in an equilibrium configuration. After these considerations we can conclude that the equilibrium in A is stable.

Conversely, a similar discussion can be done about the point B. From the picture 3.1 we infer that a displacement to the configuration B_1 leads to a gravity weaker than the internal pressure and therefore the star expands and the central density becomes lower and lower. Alternatively the displacement to the configuration B_2 provides a further contraction that indefinitely increases the central density. Therefore the equilibrium in B is unstable. Finally we can conclude that a necessary condition to the stability of a stellar equilibrium configuration is provided by

$$\frac{dM}{d\epsilon_0} > 0. \tag{3.43}$$

3.2.4 Two words on the EOS

We said that we are looking for an EOS of the form

$$P = P(\epsilon), \tag{3.44}$$

that is named a *barotropic* equation of state. However we just said that an EOS is a relation between all independent thermodynamical quantities of the system, that in general can be taken to be P, ϵ, T, N (respectively: pressure, energy

density, temperature and number of particles), because there exist well known thermodynamical relations that relates the other (such as entropy or volume) to them. Therefore a generic EOS should be of the form $f(P, \epsilon, T, N) = 0$ whereas we are looking for one of the form $f(P, \epsilon) = 0$. Let's clarify why. As already said we can consider the temperature of the star to be zero, therefore this constraint eliminates the temperature dependence. In order to eliminate the dependence on N we exploit an accidental symmetry of the Universe, i.e. the conservation of the baryon number. If we assume that the star does not contain antimatter, and that the number of mesons is negligible, the baryon number coincides with the number of baryons in the system. Since baryons are much heavier than electrons and neutrinos, the star rest mass in considered as due to baryons only. Therefore one can fix N and find that, looking at the EOS of the baryon matter, the only independent variables in the star interior are pressure and energy density. In general relativity the conservation of the baryon number can be expressed through the law ([2]):

$$(nu^{\alpha})_{;\alpha}\,, \tag{3.45}$$

where n is the baryon density and u^{α} is the 4-velocity in a LIF chosen to describe a fluid element V.

3.3 Numerical integration

For the purpose of this work it was necessary to integrate the TOV equations, therefore, in this section we review the details of the procedure and the equations of state that were employed.

As already mentioned, in order to extract a solution from the (3.37) it is necessary a numerical approach. We employed a Runge-Kutta algorithm of the fourth order to carry out the integration that was performed in the r variable.

We employ the boundary condition discussed early for the gravitational mass $M(r)$, i.e. $M(0) = 0$, but with a small modification. If we put $M(0) = 0$, from the second of the equations (3.37) comes some computational difficulties caused by the presence of the form $0/0$, and the integration doesn't start. We therefore employed, as a boundary condition for the mass, $M(r_{\varepsilon}) = (4/3)\pi r_{\varepsilon}^3$ where r_{ϵ} is taken to be small enough to not affect the final result. It was typically set to $r_{\varepsilon} = 1 \cdot 10^{-7}\, km$.

The integration was usually performed on a wide range of the central density ϵ_0 that was an input variable of the program. For each value of the central density the program proceeds through the following steps:

1. acquisition of the central energy density;

2. initialization of the initial quantities, i.e. $M(r_{\epsilon})$, ϵ_0 and P_0 (that is linked to ϵ_0 through the EOS);

3. start of the integration algorithm in r through small steps Δr;

4. when the pressure satisfies $P < P_{\min}$ the integration stops and the resultant values of M, P and R are written on an output file.

The pressure $P_{\min}$ is a limit pressure that is imposed *a priori* and such that the approximation $P_{\min} \simeq 0$ doesn't affect the result. It is chosen making some trials and analyzing when the values of the integrated quantities can be considered to be constant. It was usually put to $P_{\min} = 10^8\, dyne/cm^2$.

The integration step Δr was not taken as a constant, but since we are usually dealing with strongly variable functions, it was taken according to the formula just mentioned in the first chapter, i.e.

$$\Delta r = \Delta \cdot \left(\frac{1}{M}\frac{dM}{dr} - \frac{1}{P}\frac{dP}{dr} \right)^{-1} \tag{3.46}$$

where Δ is chosen to be $\Delta = 0.01$ in order to have a good compromise between the precision of the integration and computational speed.

The main purpose of this integration code is to allow us to study the effects that different EOSs may induce on the observable astrophysical quantities characterizing a neutron star, it is therefore important that a code like that could run with different EOSs.

In the following sections we describe the equations of state that was employed in this work and how they are implemented in the integration code.

3.3.1 Equations of states

In this work we analyze three different equations of state describing neutron star matter at zero temperature and in beta equilibrium. The same three that were employed in [6] to study the evolution of a proto-neutron star (PNS).We also employed two codes that was written by Giovanni Camelio for that paper.

The program that integrates the Tolman, Oppenheimer and Volkoff equations used in this work, is a revised version of the one written for [6]. However in order to account for the calculation of the tidal Love number, which we discuss in the following Chapter, it was necessary to modify the integration algorithm, but the way the EOSs are implemented in it is still the same of the pre-existent code.

The three different EOSs are: a mean field one, GM3; a nuclear many-body EOS based on the correlated basis functions method, CBF-EI and a model based on pure phenomenological extrapolation from the measured nuclear properties, LS-bulk. For the first two equations of state, i.e. GM3 and CBF-EI we just gave in the previous chapter an explanation of how they can be obtained.

In the GM3 EOS, baryons are described by quantum fields interacting through exchange of vector and scalar bosons (the σ, ω and ρ mesons). The equations of motion of the baryons are solved in the mean field approximation.

The CBF-EI EOS was obtained in the framework of non-relativistic many-body theory, as we saw in Chapter 2, using an improved version of the effective nuclear hamiltonian which includes the Argonne v_6' and the Urbana IX nuclear potentials.

In all EOSs the leptonic part consists of a Fermi gas of non-interacting electrons positrons and muons. The Coulomb force between protons is neglected and therefore is assumed $m_n = m_p$.

These equations of state are implemented in the TOV integration code as input files with a set of 200 tabulated values of the function $P(\epsilon)$ they predict, in the energy density range $\sim 6 \cdot 10^{13} \div 9 \cdot 10^{14}\, c^2 g/cm^3$. During the integration the program

employs these tabulated value to interpolate the value of one between the pressure and the energy density when the other is given. This interpolation is made linearly in the logarithms[1] of the quantities of interest.

The density range in which the EOSs are tabulated is however quite narrow for fully exploring the properties of neutron stars, thus for higher and smaller densities the program makes a logarithmic linear extrapolation. At small densities the extrapolation goes on until are reached the typical densities of the crust. Here the EOS is substitutes with a piecewise polytropic that models the structure of the crust. At high density the extrapolation proceeds until the speed of sound exceeds the speed of light, at this point the extrapolation is made imposing the constraint

$$c_s^2 = \frac{\partial P}{\partial \epsilon} = 1. \tag{3.47}$$

Either the crust or the causality constraint can be easily removed from the code according to the necessity of the user. In our calculations we employed both of these constraints. In figure 3.2 we can see an example of how this extrapolation works. In this picture we plotted, in the case of CBF-EI, both the EOS used for the TOV

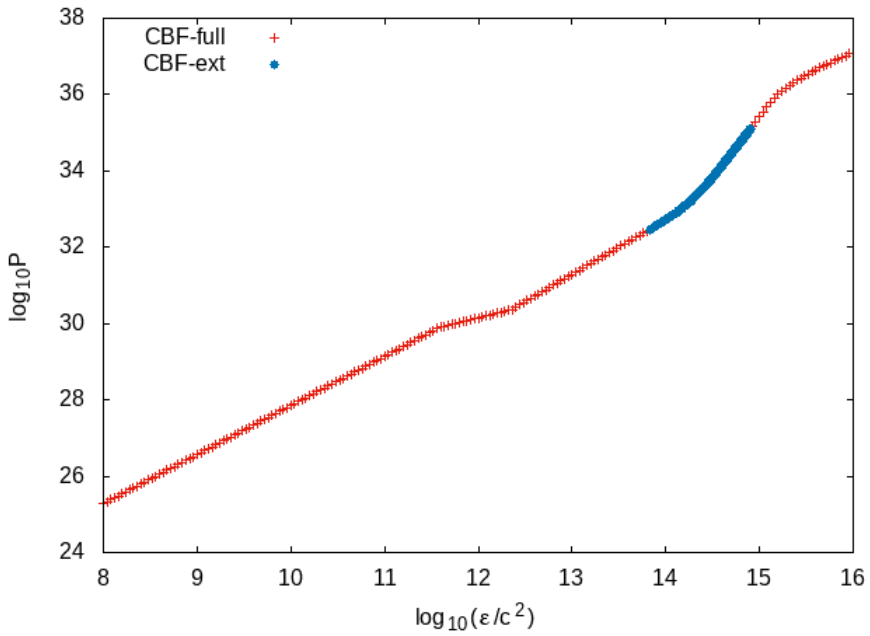

Figure 3.2. Plot of the CBF-EI full equation of state employed in the integration algorithm for the Tolman Oppenheimer and Volkoff equations.

integration in the full density range (CBF-full in the picture), and the EOS coming from the external file (CBF-ext). The figure presents a logarithmic plot, i.e. $\log P$ vs. $\log(\epsilon/c^2)$, where the quantities inside the logarithms are expresses in CGS units. We can see that the density range covered by the full EOS is far larger than the one covered by the one coming from the external file. However, as it was outlined in the previous chapter, this is compensated by the fact that there is great accordance

[1] We use base-10 logarithms.

on the equation of state of the neutron star matter at densities below the density of the atomic nuclei $\rho_0 \sim 10^{14}$. Since we plotted the logarithms in figure, and the extrapolation is linear in the logarithms, we can distinguish in the plot the parts that are subject to this extrapolation technique. In particular we can see that the EOS of the crust joins the game at densities between $\sim 10^{12}$ and $\sim 10^{13}$. Conversely we can observe a change in the slope even at densities above $\sim 10^15$ that corresponds to the causality constraint.

Since the EOS is implemented as an external input file, the code could in principle works with every EOS one wants to employ. Moreover it presents also the option to use an internal polytropic equation of state instead of an external one. This turns to be very useful in order to test its efficiency. For instance, as a first test, one could integrate the EOS characterizing a non-relativistic white dwarf, i.e. a polytropic EOS with $\Gamma = 5/3$, and find that in the density range $\rho < \bar{\rho}$ the solution of the TOV equations perfectly reproduces the one given by the non relativistic stellar structure equations[2].

Finally we report some of the results coming from our integration algorithm employing these three EOSs. In figure 3.3 the results for the mass-radius diagram, in figure 3.4 there is the plot of the compactness, M/R, in function of the central energy density ϵ_0 and in 3.5 it is shown the plot of the mass still in function of the central energy density.

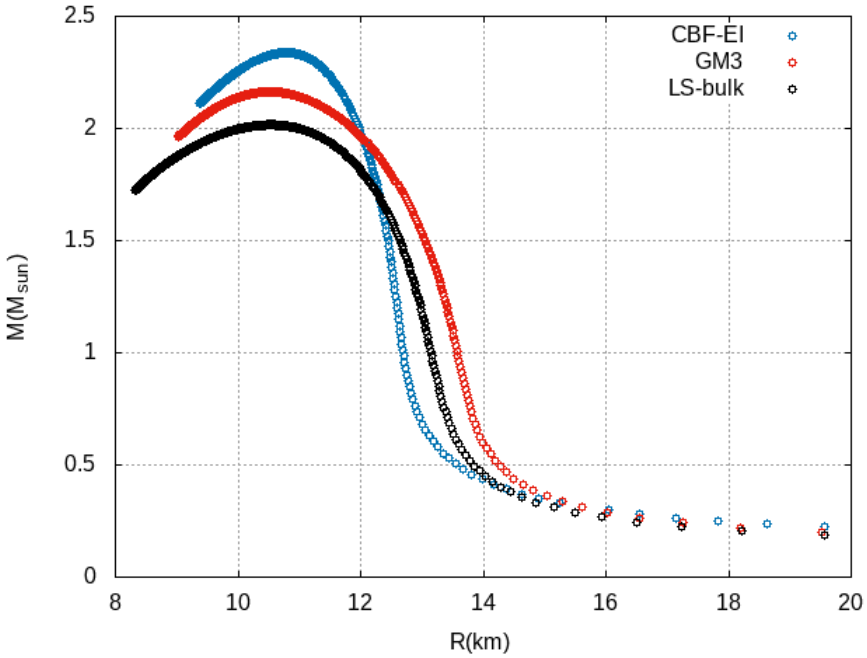

Figure 3.3. T=0 mass radius diagram for the three EOSs considered in this work. The key is shown at the top right of the figure.

[2]We outline that whereas in the newtonian case the EOS needed was $P(\rho)$, in the general relativistic regime we need $P(\epsilon)$, however, since we are considering non relativistic matter we can approx $\epsilon \simeq \rho c^2$.

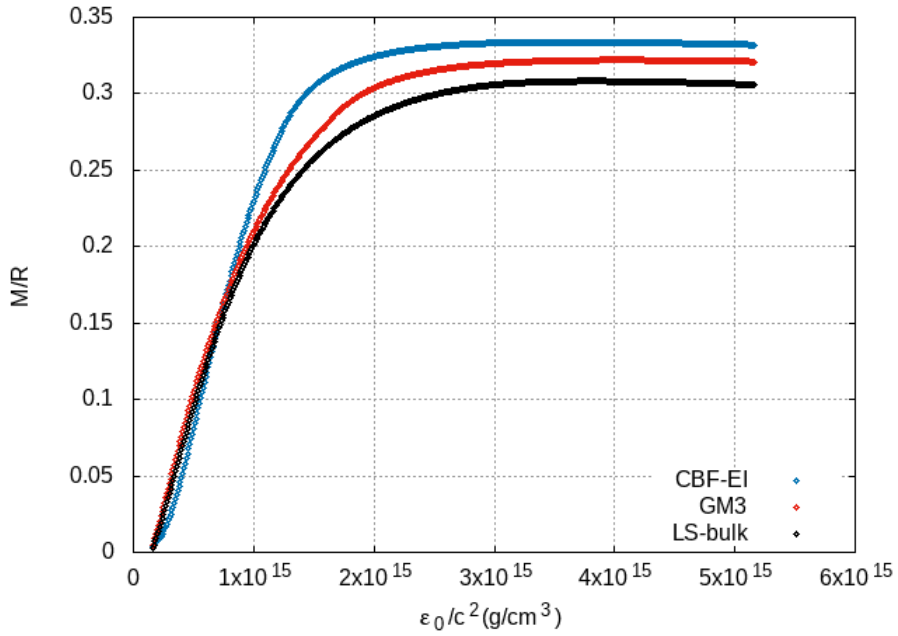

Figure 3.4. T=0 compactness-central density for the three EOSs considered in this work. The key is shown at the bottom right of the figure.

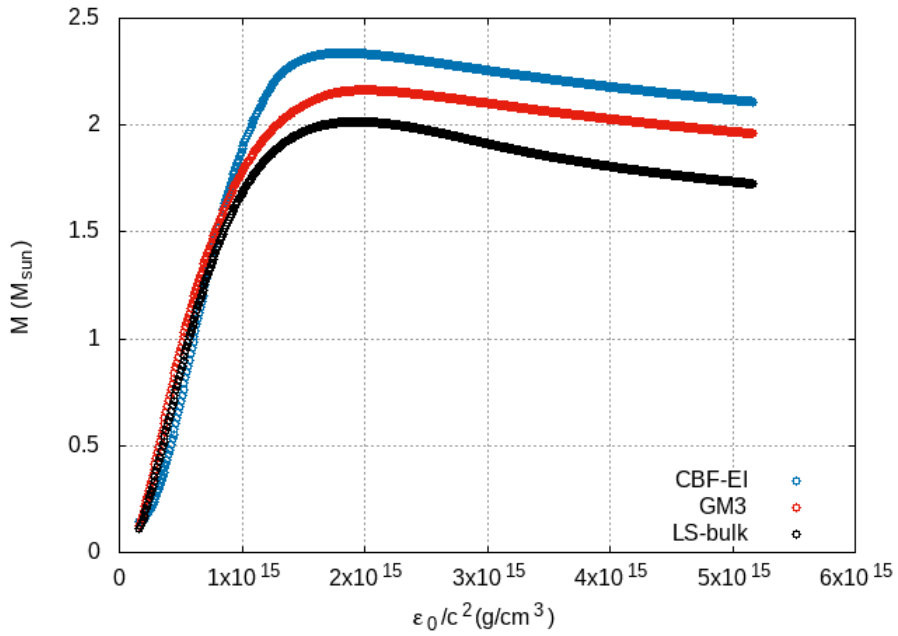

Figure 3.5. T=0 mass-central density for the three EOSs considered in this work. The key is shown at the bottom right of the figure.

Chapter 4

EOS probes in Gravitational Waves signals

Neutron stars are exceptional environments where all the four fundamental forces play a role and matter can reach densities exceeding for several times the nuclear saturation density ρ_0. We just talk about the great complexity involved in the description of how matter behaves in such extreme conditions. The theoretical efforts have also to deal with the lack of empirical data provided by the impossibility of reaching such extreme conditions in laboratory. We can therefore rely only upon astrophysical observations.

On August 17, 2017 Advanced LIGO and Advanced Virgo made the first observation of the gravitational waves signal emitted by a binary neutron-star merger. This discovery opened the door to a new frontier in the searches for EOS probes with astrophysical observations. It was shown in several works that the gravitational-wave signal coming from a binary neutron stars merger can be affected by some deformation effects, mainly due to tides and rotations. Since these effects are related to deformations they can be linked to the properties of the internal structure of the component bodies, i.e. to their equation of state and contributes to distinguish the signal provided by two neutron stars from the one of two black holes, which instead have no internal structure. Some features and techniques concerning how these effects can be seen in the gravitational waveforms, with particular attention to the high spin deformation effects, are reviewed in [1].

In this work we take in consideration only tidal effects whose relevance is quantified by the parameter known as the *tidal Love number*.

The idea is as follows. The orbital motion of binary neutron stars system produces gravitational waves that carry out energy and angular momentum from the system. This causes the decreasing of the orbital radius, and conversely the increasing in the frequency. At early times the two objects have a large orbital separations and low orbital frequencies. In this phase the bodies behave as point particles and the evolution of the frequency is primarily determined by the chirp mass $\mathcal{M}$, that is defined as:

$$\mathcal{M} = \frac{(m_1 m_2)^{3/5}}{(m_1 + m_2)^{-1/5}}, \tag{4.1}$$

where m_1 and m_2 are the two components masses. As the orbit shrinks relativistic

effects related for example to spin-orbit and spin-spin couplings become increasingly relevant.

The details about the internal structure of the two objects become important as the orbit separation approaches the size of the bodies. For neutron stars the tidal field of one of them induces a mass-quadrupole moment on the companion, which in turn generates the same effect on the other one, accelerating the coalescence. This effect is quantified by the ratio of the induced quadrupole moment to the external tidal field, that is proportional to the tidal deformability

$$\Lambda = \frac{2}{3} k_2 \left(\frac{c^2 R}{Gm} \right)^5 , \tag{4.2}$$

where R and m are respectively the radius and the mass of the star, whereas k_2 is the second tidal Love number. For any given stellar mass, R and k_2 are uniquely determined by the EOS of the neutron-star matter. Tidal effects are predicted to become relevant near frequencies $f_{GW} \simeq 600\, Hz$, therefore their are potentially observable, even if at these frequencies the stars are close to merge and the sensitivity of the instruments has begun to decrease. Experimentally the properties of the gravitational-wave sources are inferred by matching the data with predicted waveforms.

We will not go into details about how tidal deformations affect the waveform of the measured gravitational wave signals. We are much interest in the definition and the calculations of the tidal Love number for the three different EOSs that was early examined. Finally we will compare our results to the experimental data coming from the LIGO-VIRGO collaboration that are analyzed in [7] and [8].

4.1 Tidal Love number

From now on we will use geometric units, even if in some cases we will explicit the gravitational constant G.

4.1.1 Newtonian theory

A tide is a deformation effect induced on a body by another because of the variation of the gravitational force that acts on it [9]. If we consider a quadrupolar tidal field, its effect on its companion is characterized by the quantity $\mathcal{E}_{ij}$, named as *tidal momentum* and defined as (see [10])

$$\mathcal{E}_{ij} = - \left. \frac{\partial^2 \Phi_{\text{ext}}}{\partial x_i \partial x_j} \right|_{\vec{x}=\vec{x}_{\text{c}}} , \tag{4.3}$$

where i and j ranging from 1 to 3, Φ_{ext} in the newtonian external potential and $\vec{x}_{\text{c}}$ labels the position of the center of mass of the body subject to the tidal field.

Let us see it in more details. If we consider a non rotating spherical object, A, subject to a gravitational field provided by a point-like source, B, at distance a from the center of mass of A. We are interest in the force that acts on a point P, with

mass m_P, on the surface of A. We can therefore write the equation of motion for P in a generic reference frame as

$$m_P \vec{a}_P = -g_A m_P \cdot \hat{u}_P + \vec{F}_{AB} = -g_A m_P \cdot \hat{u}_P - m_P \vec{\nabla} \Phi(\vec{r}_P). \tag{4.4}$$

In the above equation g_A is the surface gravity acceleration of A, $\vec{r}_P$ is the position of P, $\Phi(\vec{r}_P)$ is the gravitational potential induced by B in the point $\vec{r}_P$ and $\hat{u}_P$ is given by

$$\hat{u}_P = \frac{\vec{r}_P - \vec{r}_c}{|\vec{r}_P - \vec{r}_c|} \tag{4.5}$$

with $\vec{r}_c$ being the position of the center of mass of A. We can now expand the gradient of $\Phi(\vec{x})$ around $\vec{x} = \vec{r_c}$ and keeping only the first two terms we find[1]:

$$\frac{\partial \Phi}{\partial x_i} \approx \left.\frac{\partial \Phi}{\partial x_i}\right|_{r_c} + \left.\frac{\partial^2 \Phi}{\partial x_j \partial x_i}\right|_{r_c} (\vec{x} - \vec{r_c})_j = \left.\frac{\partial \Phi}{\partial x_i}\right|_{r_c} - \mathcal{E}_{ji} (\vec{x} - \vec{r_c})_j \,. \tag{4.6}$$

If we now put ourselves in the mass-centered reference frame of the body A and neglect the effects of rotations (both around the symmetry axis of the body and around the center of mass of the system A+B) we find that the tidal force, i.e the force that is not given to the own gravity of the body A, that acts on P is given by:

$$F_i^{\text{tidal}} = m_P x_j \mathcal{E}_{ji.} = -m_P \frac{\partial \Phi^{\text{tidal}}}{\partial x_i} \tag{4.7}$$

where now we label with x_i the position in the mass-centered reference frame and we defined a tidal potential whose minus gradient gives rise to the tidal force F^{tidal}:

$$\Phi^{\text{tidal}} = \frac{1}{2} x_i x_j \mathcal{E}_{ij.} \tag{4.8}$$

The tidal moment $\mathcal{E}_{ij}$ is a symmetric tensor, and since the gravitational potential satisfies the Laplace equation in vacuum it is also tracefree, therefore it is a symmetric tracefree (STF) tensor. Since we have a quadrupolar external tidal potential we expect that the body will develop a quadrupolar deformation, i.e. it will acquire a mass quadrupole moment Q_{ij}. The quadrupole moment is given by:

$$Q_{ij} = \int d^3x \, \rho(\vec{x}) \left(x_i x_j - \frac{1}{3} r^2 \delta_{ij} \right), \tag{4.9}$$

where ρ is the mass density, x_i is the i-th coordinate of a point in the space with respect to the reference frame sets in the center of mass of the body, and r is defined through $r^2 = (\delta_{ij} x_i x_j)$. We also remark that Q_{ij} is another STF tensor.

In the case of a weak tidal field we will have a linear relation between Q_{ij} and $\mathcal{E}_{ij}$ i.e.

$$Q_{ij} = -\lambda \mathcal{E}_{ij} \tag{4.10}$$

[1]Keeping only the first two terms, i.e. truncate the expansion to $O(x)$, means that we can consider the radius of the body to be small enough to allow a linear approximation of the external field.

and by dimensional analysis follows that

$$\lambda = \frac{2}{3} k_2 R^5 G^{-1} \tag{4.11}$$

where R is the star's radius, the factor $2/3$ is a convention and the dimensionless constant k_2 is the second tidal Love number that quantifies the quadrupolar tidal deformation.

Using these expressions we can write the potential outside the body as a sum of the body and external potentials that result to be

$$\Phi_{\text{tot}} = -\frac{M}{r} - \frac{3}{r^5} Q_{ij} x_i x_j + \frac{1}{2} \mathcal{E}_{ij} x_i x_j. \tag{4.12}$$

In this last equation the total potential was truncated to the leading, quadrupole order in a Taylor expansion of both the external and the body potential. The first two terms account for the potential generated by the deformed object, indeed it presents a monopole and a quadrupole terms, whereas the third term accounts for the external tidal potential.

Substituting (4.10) and (4.11) into (4.12) we finally find:

$$\Phi_{\text{tot}} = -\frac{M}{r} + \left[\frac{2k_2}{G} \left(\frac{R}{r} \right)^5 + \frac{1}{2} \right] \mathcal{E}_{ij} x_i x_j. \tag{4.13}$$

4.1.2 Relativistic theory

In the previous section we derived the expression of the total newtonian potential in the case of an body subject to a quadrupolar tidal field, obtaining Eq. (4.12). Since we are interest in the calculation of the Love number for a neutron star we have to transpose the previous discussion in the framework of general relativity. At this purpose, we remind that in the weak field limit holds the identity

$$\Phi = -\frac{(1 + g_{00})}{2}, \tag{4.14}$$

which can be used to define the quantities Q_{ij} and $\mathcal{E}_i j$ in general relativity. Indeed, combining (4.12) and (4.14), in the weak field limit, we find:

$$-\frac{(1 + g_{00})}{2} = -\frac{M}{r} - \frac{3}{r^5} Q_{ij} x_i x_j + O\left(\frac{1}{r^3}\right) + \frac{1}{2} \mathcal{E}_{ij} x_i x_j + O\left(r^3\right) \tag{4.15}$$

where Q_{ij} and $\mathcal{E}_{ij}$ are given respectively by (4.9) and (4.3). Nevertheless we are interest in fully relativistic stars which requires going beyond newtonian physics. In the strong field case the equations (4.9) and (4.3) are no longer valid, but the expansion (4.15) still holds in the asymptotically flat region in the star local rest frame and serves to define the moments Q_{ij} and $\mathcal{E}_{ij}$. In the following we follow the approach of [11] and [12] in order to carry out the relativistic expression of the tidal Love number for an $l = 2$ perturbation: k_2.

First of all we note that since Q_{ij} and $\mathcal{E}_{ij}$ are STF tensors we can decompose them into:

$$Q_{ij} = \sum_{m=-2}^{2} \mathcal{E}_m \mathcal{Y}_{ij}^{2m}, \tag{4.16}$$

$$\mathcal{E}_{ij} = \sum_{m=-2}^{2} Q_m \mathcal{Y}_{ij}^{2m}, \tag{4.17}$$

where $\mathcal{Y}_{ij}^{2m}$ are defined as the symmetric tracefree tensors that satisfy

$$Y_{2m}(\theta, \phi) = \mathcal{Y}_{ij}^{2m} n_i n_j \tag{4.18}$$

with $\vec{n}$ being the unit vector of a generic point in the three-dimensional space, $\vec{n} = (\sin\theta\cos\phi, \sin\theta\sin\phi, \cos\theta)$, and the sum over the indices i and j is understood. Equation (4.10) can therefore be written as:

$$Q_m = -\lambda \mathcal{E}_m \tag{4.19}$$

and without loss of generality, we can assume that only one $\mathcal{E}_m$ is nonvanishing, since this is sufficient to compute λ.

In order to find the expression for k_2 in general relativity we begin examining the behavior of the equilibrium configuration under linearized perturbations due to an external quadrupolar tidal field, following [11][13]. The full metric of the spacetime is given by

$$g_{\alpha\beta} = g_{\alpha\beta}^{(0)} + h_{\alpha\beta}, \tag{4.20}$$

where $h_{\alpha\beta}$, with $|h_{\alpha\beta}| << 1$, is a metrics perturbation and $g_{\alpha\beta}^{(0)}$ is the metrics of a stationary, spherically symmetric spacetime given by (3.31). The angular dependence of $h_{\alpha\beta}$ is analyzed into spherical armonics and are taken into consideration only the $l = 2$, static, even-parity perturbations in the Regge-Wheeler gauge. According to [11], under these hypothesis $h_{\alpha\beta}$ can be written as

$$h_{\alpha\beta} = Y_{2m}(\theta, \phi) \begin{pmatrix} -e^{2\nu(r)} H_0(r) & 0 & 0 & 0 \\ 0 & e^{2\lambda(r)} H_2(r) & 0 & 0 \\ 0 & 0 & r^2 K(r) & 0 \\ 0 & 0 & 0 & r^2 \sin^2\theta K(r) \end{pmatrix}. \tag{4.21}$$

We want to solve the linearized Einstein equations

$$\delta G_{\nu}^{\mu} = 8\pi \delta T_{\nu}^{\mu}. \tag{4.22}$$

We can write the variation of the stress-energy tensor as:

$$\delta T_{\nu}^{\mu} = \mathrm{diag}\left(-\delta\epsilon,\, \delta P,\, \delta P,\, \delta P\right), \tag{4.23}$$

where, since $P = P(\epsilon)$ therefore

$$\delta\epsilon = \left(\frac{dP}{d\epsilon}\right)^{-1} \delta P. \tag{4.24}$$

Using equations (4.20) and (4.21) one can calculate the components of δG_{ν}^{μ} and put them, together with (4.23), into (4.22). After some calculations one finds that all the radial functions in the metrics perturbation $h_{\alpha\beta}$ can be related to a unique function $H(r) \equiv H_0(r)$ that obeys the following differential equation

$$\begin{aligned} &H'' + H' \left\{ \frac{2}{r} + e^{2\lambda} \left[\frac{2M(r)}{r^2} + 4\pi r(P - \epsilon) \right] \right\} + \\ &+ H \left[-\frac{6e^{2\lambda}}{r^2} + 4\pi e^{2\lambda} \left(5\epsilon + 9P + \frac{\epsilon + P}{dP/d\epsilon} \right) - (2\nu')^2 \right] = 0 \end{aligned} \tag{4.25}$$

where we labeled d/dr with the prime. We can find the boundary conditions for the previous differential equation requiring regularity of H at $r = 0$ and solving for H near $r = 0$. This yields

$$H(r) = a_0 r^2 \left\{ 1 - \frac{2\pi}{7} \left[5\epsilon(0) + 9P(0) + \frac{\epsilon(0) + P(0)}{(dP/d\epsilon)(0)} \right] r^2 + O(r^3) \right\} \tag{4.26}$$

where a_0 is a constant that can be eliminated using continuity of H and its derivative across $r = R$. However for our purpose, which concerns the numerical integration of (4.25), we will see that the value of the parameter a_0 is insignificant. We remind that our goal now is to define the quantities Q_{ij} and $\mathcal{E}_{ij}$ through the asymptotic expansion of (4.15), therefore we want to find $H(r)$ outside the star. In this region the metrics of the unperturbed spacetime is given by the Schwarzschild solution and the components of the stress-energy tensor are all zero. Eq. (4.25) therefore becomes

$$H'' + \left(\frac{2}{r} - \lambda' \right) H' - \left(\frac{6e^{2\lambda}}{r^2} + (2\lambda')^2 \right) H = 0. \tag{4.27}$$

We remind that in the Schwarzschild solution λ and ν satisfies:

$$e^{2\nu} = 1 - \frac{2M}{r}, \tag{4.28}$$

$$e^{2\lambda} = \frac{1}{1 - \frac{2M}{r}}. \tag{4.29}$$

With the change of variable $x = (r/M - 1)$ Eq. (4.27) can be turned into the form of the associated Legendre equation with $l = m = 2$

$$\left(x^2 - 1 \right) H'' + 2xH' - 6 \left(6 + \frac{4}{x^2 - 1} \right) H = 0. \tag{4.30}$$

The general solution of the above equation is written in terms of the associated Legendre functions $Q_2^2(x)$ and $P_2^2(x)$ as

$$H = c_1 Q_2^2(x) + c_2 P_2^2(x) \tag{4.31}$$

where c_1 and c_2 are two coefficients to be determined. After substituting the explicit form of the associated Legendre functions from [14], into (4.31) and performing an asymptotic expansion for large r we obtain the following expression for $H(r)$:

$$H(r) = \frac{8}{5} \left(\frac{M}{r} \right)^3 c_1 + O\left(\left(\frac{M}{r} \right)^4 \right) + 3 \left(\frac{r}{M} \right)^2 c_2 + O\left(\frac{r}{M} \right), \tag{4.32}$$

where the coefficients c_1 and c_2 can now be determined by matching Eq. (4.32) with the asymptotic expansion (4.15), remembering that $H \equiv H_0$ is linked to the metrics perturbation h_{00} that appears in (4.15) because $g_{00} \approx g_{00}^{(0)} + h_{00}$. Using also (4.19) we find that the coefficients c_1 and c_2 are given by:

$$c_1 = \frac{15}{8} \frac{1}{M^3} \lambda \mathcal{E}, \quad c_2 = \frac{1}{3} M^2 \mathcal{E}. \tag{4.33}$$

Finally one can solve the explicit form of Eq. (4.31) for λ in terms of H and its derivative at the star's surface, i.e. at $r = R$ and, using (4.11), the tidal Love number k_2 can be carried out and results to be

$$\begin{aligned} k_2 = {} & \frac{8C^5}{5}(1-2C)^2\left[2+2C(y-1)-y\right]\cdot \\ & \cdot\Big\{2C\left[6-3y+3C(5y-8)\right]+4C^3\Big[13-11y+C(3y-2)+2C^2(1+y)\Big]+ \\ & +3(1-2C)^2\left[2-y+2C(y-1)\right]\log(1-2C)\Big\}^{-1}, \end{aligned} \tag{4.34}$$

where it was defined the quantities C and y as

$$C = \frac{M}{R}, \quad y = \frac{RH'(R)}{H(R)}. \tag{4.35}$$

This result tells us that the ingredients we need in order to evaluate the tidal Love number k_2 are the star compactness and the quantity y that can be computed by integrating Eq. (4.25) in the region $0 < r < R$. We note that (4.25) depends on quantities that are determined by solving the unperturbed problem i.e. by the solution of the TOV equations. Therefore to evaluate y and C we have to integrate simultaneously the TOV equations and Eq. (4.25).

4.2 Tidal Love number calculation and results

In this section we review how we implemented the calculation of the Tidal Love number in our TOV integration algorithm. First of all we note that the differential equation for $H(r)$ depends on quantities that can be calculated in the usual TOV integration code. An integration algorithm of a differential equation system:

$$\frac{d\vec{y}}{dx} = \vec{f}(\vec{y}, x), \tag{4.36}$$

calculates the quantities of interest, i.e. the components $y_i(x)$, thorough a series of steps in which the independent variable, x, is always increased by a little quantity h, and $y_i(x+h)$ is calculated employing an approximation. For example one can use

$$y(x+h) \approx y(x) + y'(x)h. \tag{4.37}$$

The approximation thorough which one calculates the quantity $y(x+h)$ defines the integration algorithm. Equation (4.37) defines the simplest integration algorithm, known as Euler algorithm. Clearly, since we are recurring to a discrete approximation, the final result will be affected by an error. For example, it is clear that approximating with (4.37) we will make an error on a single step, of order $O(h^2)$. If we are integrating x in a range that is $\Delta x = L$ wide, the final error will be $O(h^2)$ multiplied by the number of steps $N_{step} = L/h$, i.e. we will have an overall error of $O(h)$. The better is the algorithm the smaller will be the error. As already said we employ the well known 4-th order Runge-Kutta algorithm that will bring an overall error of order $O(h^4)$. Looking at the example of (4.37), in order to compute the value of y after

increasing x of a step h, we need to know the value of y at the previous step. This tells us that we can't proceed to the integration without an initial condition on the y. This considerations can be easily extended to the case of differential equation system such as (4.36).

Coming back to our case, we have an algorithm that integrates the TOV equations, therefore we know, step for step all the quantities that appears in the differential equation (4.25): $M(r)$, $P(r)$ and $\epsilon(r)$ are given by integrating the system (3.37) plus the equation of state $P(\epsilon)$; ν' and λ are instead respectively given by equations (3.36) and (3.38). We can therefore integrate (4.25) together with the TOV equations as it was an unique big differential equation system of the form given by (4.36). However the one in Eq. (4.36) is a system of the first order, i.e. in it appear only first derivatives, therefore, in order to have a system of such a form, we have to transform Eq. (4.25) into two coupled differential equations of the first order thus, naming $F \equiv H'$, we have

$$\begin{cases} H' = F \\ F' = -F\left\{\dfrac{2}{r} + e^{2\lambda}\left[\dfrac{2M(r)}{r^2} + 4\pi r(P-\epsilon)\right]\right\} + \\ \quad - H\left[-\dfrac{6e^{2\lambda}}{r^2} + 4\pi e^{2\lambda}\left(5\epsilon + 9P + \dfrac{\epsilon+P}{dP/d\epsilon}\right) - (2\nu')^2\right] = 0. \end{cases} \tag{4.38}$$

The only thing left to do is to impose an initial condition on H and H'. To this purpose, if we put it to be near $r = 0$, we can use the expansion of equation (4.26). Keeping only the first term we have, for $r_0 \sim 0$:

$$\begin{aligned} H(r_0) &= a_0 r_0^2 \\ H'(r_0) &= 2a_0 r_0. \end{aligned} \tag{4.39}$$

The constant a_0 is in principle unknown unless one knows the complete analytical solution, however for our purpose it is insignificant and we put its value to $a_0 = 1$. To understand why a_0 plays no role we need only to consider that k_2 depends on the ratio H'/H i.e. it is insensible to a rescale of H and H' by the same constant.

In order to test the goodness of the integration program it was first of all used to compute the Love number for a polytropic EOS with different values of the polytropic index n, that is linked to the adiabatic index Γ through

$$\Gamma = 1 + \frac{1}{n}. \tag{4.40}$$

The obtained results are reported in the table 4.1, and can be compared with that obtained in the paper of Tanja Hinderer [11].

Before going on we underline another difficulty that arise when one takes into consideration an equation of state that is not a polytropic. In Eq.(4.38) we can see that the differential equation for H' depends on the quantity $dP/d\epsilon$. Since, as it was already said, an EOS that is not a polytropic is implemented in the computational algorithm as an input files with a series of tabulated values, in order to calculate the derivative of the pressure we have to do another discrete approximation. We

Table 4.1. Table of the resulting Love numbers (k_2) for polytropic EOSs with polytropic index labeled by n. The values obtained in this work are compared with that carried out in the paper [11], that are labeled by k_2' in the table.

n	M/R	k_2	k_2'
0.3	0.1	0.285	0.294
0.3	0.15	0.194	0.201
0.3	0.2	0.125	0.119
0.5	0.1	0.228	0.230
0.5	0.15	0.153	0.158
0.5	0.2	0.0967	0.095
0.5	0.25	0.0562	0.0569
0.7	0.1	0.179	0.1779
0.7	0.15	0.118	0.1171
0.7	0.2	0.0730	0.0721
0.7	0.25	0.0408	0.042
1.0	0.1	0.123	0.122
1.0	0.15	0.0783	0.0776
1.0	0.2	0.0459	0.0459
1.0	0.25	0.0234	0.0253
1.2	0.1	0.0941	0.0931
1.2	0.15	0.0580	0.0577
1.2	0.2	0.0323	0.0327

Table 4.2. Tidal love number k_2 for three different EOS of nuclear matter

EOS	M/R	k_2
CBF-EI	0.101	0.0901
CBF-EI	0.150	0.0808
CBF-EI	0.200	0.0589
CBF-EI	0.249	0.0373
CBF-EI	0.300	0.0192
GM3	0.101	0.104
GM3	0.150	0.0835
GM3	0.202	0.0549
GM3	0.251	0.0316
GM3	0.300	0.0150
LS-bulk	0.100	0.104
LS-bulk	0.149	0.0850
LS-bulk	0.201	0.0558
LS-bulk	0.250	0.0318
LS-bulk	0.300	0.0125

computed the derivative of $d\log P/d\log\epsilon$ as the incremental ratio, i.e. we made the approximation

$$\frac{d\log P}{d\log\epsilon} \approx \frac{\Delta\log P}{\Delta\log\epsilon} \tag{4.41}$$

and then we computed the derivative of the pressure through:

$$\frac{dP}{d\epsilon} = \frac{P}{\epsilon}\cdot\frac{d\log P}{d\log\epsilon} \approx \frac{P}{\epsilon}\cdot\frac{\Delta\log P}{\Delta\log\epsilon}. \tag{4.42}$$

If we look at the Figure 3.2 we can see that the EOS in the most of its range is linear in the logarithms, and where it is not we can see that the slope is never too much steep, therefore we can think that our approximation for the calculation of $dP/d\epsilon$ can be quite good. However for equations that are not polytropic (which are clearly linear in the logarithms) we observe small fluctuations on the third significant digit when we vary the number of points with which we make the discretization of the EOS in order to calculate the derivative of the pressure with respect to the energy density. For this reason we outline our purpose to make an improved version of this first algorithm as soon as possible.

Finally we propose the graphics that show the behavior of the k_2 with respect to the compactness and to the mass for the three EOSs analyzed in this work. The plots show only the values corresponding to stable stars, i.e. those configurations that in the $M(R)$ plot are on the right of the maximum. In the top two panels of the figure 4.1 are represented the functions $k_2(M/R)$ (left panel) and $k_2(M)$ (right panel), for CBF-EI (red), GM3 (blue) and LS-bulk (black triangles). In the bottom panel we still plotted $k_2(M/R)$ but with the addition of some polytropic EOSs with different values of the polytropic index n. The same plot is impossible for $k_2(M)$ since for the polytropic case it depends also from the multiplying constant K. This

is not the case for $k_2(M/R)$. We remind that we included the crust in the EOSs that are not polytropics.

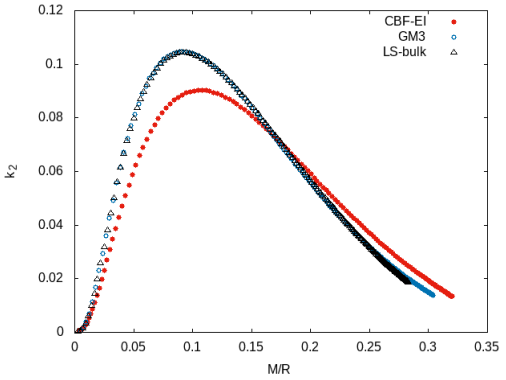

(a) $k_2(M/R)$

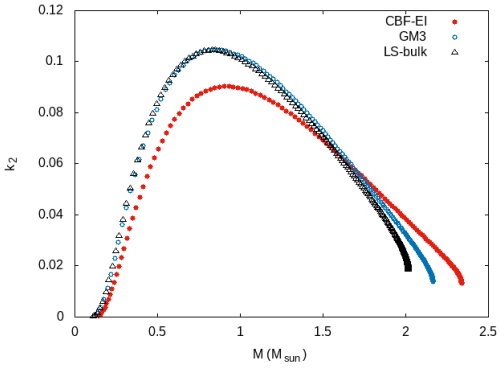

(b) $k_2(M)$

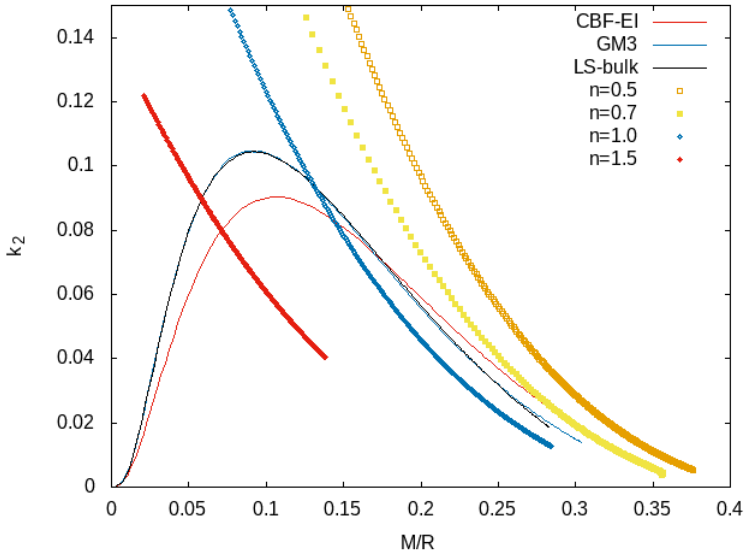

(c) $k_2(M/R)$ with also polytropic EOSs

Figure 4.1. The figure shows in the top panel the functions $k_2(M/R)$ (a) and $k_2(M)$ (b) for the three EOSs: CBF-EI (red solid balls), GM3 (blue hollow balls) and LS-bulk (black triangles). In the bottom panel it is shown the function $k_2(M/R)$ for the same three EOSs and presents the addition of the behavior of some polytropic EOSs with different values of the polytropic index n as it is labeled in the key.

We now briefly discuss this figure and remind that a similar treatment for other EOSs was already done in [12]. Let us consider Fig. 4.1 (c). The tidal Love number, being the ratio between the quadrupole moment induced by the external tidal field and the tidal field itself, represent how easily the bulk of the star is deformed under tidal effects. The larger is the deformation (i.e. the value of the quadrupole moment), the higher will be k_2. If most of the star's mass is concentrated at the center (centrally condensed), the tidal deformation will be smaller. The figure shows

that, for fixed compactness the tidal Love number decreases as the polytropic index n increases. It is expected since the polytropic index measures the stiffness of the matter, as explained in Chapter 1. Higher n corresponds to a more compressible matter, i.e. it will be more centrally condensed and therefore is more difficult to induce a large tidal deformation on it. Fixing n we see that the tidal Love number still decreases. Indeed it is in some sense intuitive that a more compact star will not be largely deformed. We note also that the tidal Love number tends to zero for compactness near the one of a black hole, $M/R = 0.5$ (since the radius of a black hole can be identified with its event horizon i.e. R=2M). We note that our three different EOSs behaves like a polytropic for high compactness, whereas for small compactness, k_2 reaches a maximum and then decreases. This can be read as the fact that the EOSs accounts for the formation of a soft crust at densities below ρ_0. For small compactness the crust becomes a larger fraction of the star matter thus the star becomes more centrally condensed and therefore it is less deformed. We can qualitatively understand it as follows. If we look at the plot M/R vs ϵ_0 (Fig. 3.4), we can see that compactness between 0 and 0.5 correspond to central densities in the range $9 \cdot 10^{14} \div 1 \cdot 10^{15}\, g/cm^3$. If we keep in mind the form of the EOS illustrated in Fig. 3.2, we can see that at densities in the range of $10^{14} \div 10^{15}\, g/cm^3$ the slope of the EOS becomes more steep. Therefore as the compactness grows, in the same way grows the contribute of the part that have a slope more steep, i.e. that can be parameterized with a polytropic index that is smaller then the one associated to a more soft slope. Therefore, while in a polytropic the grows of compactness leads to a decreasing in the Love number, in the case of an EOS, such as the one in 3.2, it leads also to an increasing in the contribute of regions that can be parameterized with a smaller polytropic index. This leads the love number to increase. This increasing proceeds till the Love number reaches its maximum value an then it starts to decrease with a profile that finally can be approximated with a polytroipic.

4.2.1 Experimental observations

On August 17, 2017, the LIGO and VIRGO detector network observed a gravitational-wave signal from the inspiral of two compact objects, consistent with a binary neutron star system (BNS). The contribute arising from the presence of VIRGO was determinant in order to strongly constraint the sky location of the source. The combined data from LIGO and VIRGO identified a precise sky location to an area of 28 $\deg^2$. This measurement enabled strong searches for an electromagnetic counterpart that was finally identified in a sky region consistent with the one inferred for the gravitational-waves source. The detection of a gravitational-wave signal is done through a matched filtering procedure, i.e. the data coming from the detectors are matched together with a theoretical predicted waveform, $h(t, \vec{\theta})$ that depends on time, t, and on a set of parameters characterizing the source, $\vec{\theta}$. Therefore a GW detection proceeds through the identification of a particular pattern inside the rough signal coming from the detectors. For the details about the analysis techniques and results carried out in this experiments we invite the reader to consult [7]. We limit ourselves to outline their following results. The chirp mass, that is the best measured combination of masses in a gravitational-wave signal, was established to

be $\mathcal{M} = 1.188^{+0.004}_{-0.002} M_\odot$. While the chirp mass is well constrained, the estimates on the component masses, m_1 and m_2 (with $m_1 \geq m_2$) are affected by the degeneracy between the mass ratio q and the aligned spin of the two components χ_{1z} and χ_{2z}[2]. Therefore the values of the component masses and q depends on the assumptions made on the component spins. In the data analysis where analyzed two cases: high spin case, $|\chi| \leq 0.89$ and low spin case, $|\chi| \leq 0.05$. The hypothesis on the spin leads to constraint into an interval the values of the component masses. For the high spin scenario it was found: $m_1 \in (1.36, 2.26) M_\odot$ and $m_2 \in (0.86, 1.36) M_\odot$. Conversely for the low spin scenario it was found $m_1 \in (1.36, 1.60) M_\odot$ and $m_2 \in (1.17, 1.36) M_\odot$. All these bounds are 90% posterior probability intervals. In figure 4.2 we report the resulting posterior probabilities that was found in [7] for both high and low spin cases.

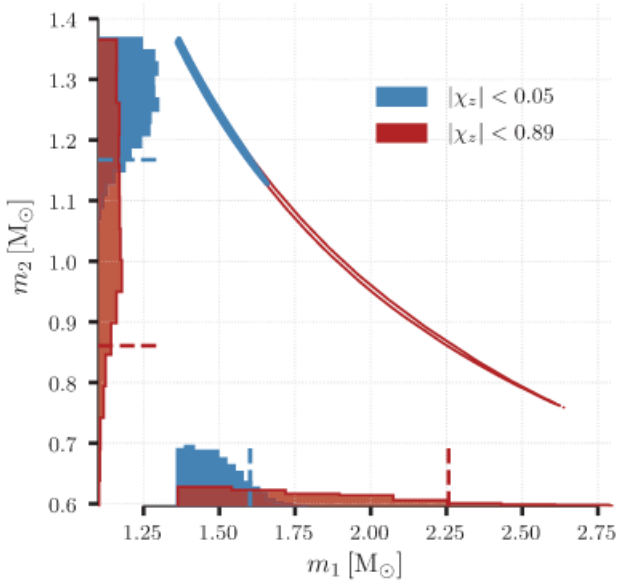

Figure 4.2. Two dimensional posterior probability distribution for the component masses m_1 and m_2 in the rest frame of the source in the low spin scenario ($|\chi| < 0.05$, blue) and the high spin scenario ($|\chi| < 0.89$, red). The shape of the joint posterior probability density function is determined by a line of constant $\mathcal{M}$ and its width is given by the uncertainty on $\mathcal{M}$. On the two axis are shown the marginalized one dimensional posterior probabilities for the two component masses independently.

They made also a similar analysis for the tidal deformability of each component of the binary system, Λ_1 and Λ_2. The tidal deformability is linked to the tidal Love number through

$$\Lambda = \frac{2}{3} k_2 \left(\frac{R}{M} \right)^5 . \tag{4.43}$$

It can be shown that to the leading order in Λ_1 and Λ_2 the gravitational-wave

[2]With χ_z we label the dimensionless spin component along the total orbital angular momentum of the binary system. The dimensionless spin is the ratio between the measured angular momentum and the maximum angular momentum allowed by the mass of the body

phase is influenced by the parameter

$$\tilde{\Lambda} = \frac{16}{13}\frac{(m_1 + 12m_2)m_1^4\Lambda_1 + (m_2 + 12m_1)m_2^4\Lambda_2)}{(m_1 + m_2)} \tag{4.44}$$

Assuming a uniform prior on $\tilde{\Lambda}$ it was constrained to $\tilde{\Lambda} \leq 800$ in the low spin case and $\tilde{\Lambda} \leq 700$ in the high spin case. With this constraint it was found the two-dimensional posterior distribution function for the two tidal deformabilities Λ_1 and Λ_2 in the two spin scenarios. This is plotted in Fig. 4.3 (taken from [7]), together with the curves predicted by a set of different equations of state for stars with masses compatible with the posterior distribution functions shown in Fig. 4.2. This is done under the hypothesis that both the objects in the binary systems are neutron stars described by the same equation of state.

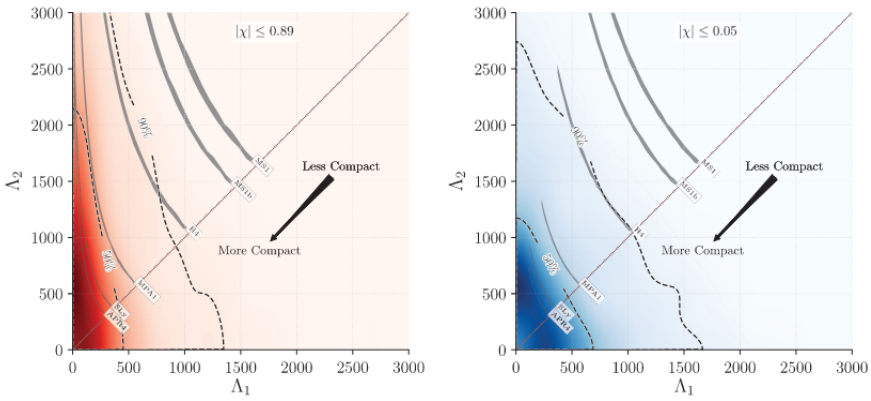

Figure 4.3. Probability density for the tidal deformability parameters of the two component stars inferred from the detected signals taken from [7]. The dashed lines represent the boundaries enclosing 90% and 50% of the probability density. The diagonal dashed lines represent the $\Lambda_1 = \Lambda_2$ boundary. The constraints are shown in the two spin scenarios. In the left panel we have the high spin case ($|\chi| \leq 0.89$), whereas in the right panel is shown the low spin scenario ($|\chi| \leq 0.05$). As a comparison the authors have plotted also the prediction for the tidal deformabilities of a set of equations of state. The EOSs that are outside the 90% region, which predict less compact stars, are disfavored by the constraints found in that work.

This kind of analysis was improved in [8] where the authors have also estimated the value of the radius for each of the two component objects following two different methods. One employs the use of equation-of-state insensitive relations between various macroscopic properties of the neutron stars; the other one is instead based on an efficient parameterization of the EOS itself constrained by the measured data. For the detail of such analysis we remind to the paper mentioned above, here we limit ourselves to report their results. From the LIGO and VIRGO data alone, and following the first method they have measured the two neutron star radii as $R_1 = 10.8^{+2.0}_{-1.7}\,km$, for the heavier star and $R_2 = 10.7^{+2.1}_{-1.5}\,km$, for the lighter star. Employing the second method, with the further requirement that the parameterized EOS will support masses larger than $1.97M_\odot$[3], it was found $R_1 = 11.9^{-1.4}_{+1.4}\,km$ and

[3]This value is chosen as $1-\sigma$ conservative estimate, based on the observation of PSRJ0348+0432 with $M = 2.01 \pm 0.04\,M_\odot$, the heaviest neutron star known to date.

$R_2 = 11.9^{+1.4}_{-1.4}\,km$. All these values are given at 90% credible level. Finally they also constrained the function $P(\rho)$, where ρ is the rest-mass density, with pressure at twice nuclear saturation density measured at $3.5^{+2.7}_{-1.7} \cdot 10^{34} dyne\, cm^{-2}$ at 90% credible level.

4.2.2 Confrontation with our results

In our work we used the data of [7] regarding the low spin scenario to test the predictions made by the three EOSs we took into consideration. We aim to use our code in order to generate couples of stars, with masses m_1 and m_2, distributed in a way consistent with the joint probability distribution shown in figure 4.2 in the low spin case. Since our code computes the tidal Love number allowed by the equilibrium configuration arising at the end of the integration, once we have couples of stars distributed as in Fig. 4.2 we are therefore able to draw a prediction for the function $\Lambda_1(\Lambda_2)$, that can be compared with the constraints given in Fig. 4.3. However, since the initial condition of our integration code is the central density ϵ_0 and not the final mass of the star, in order to reproduce a star with a given mass m, for each EOS employed in the code, we have to know the value of the central density that allows the formation of a star of such a mass. In order to do that we first of all performed the integration of TOV equations in a wide range of the central density ϵ_0. For each EOS now we have a tabulated function $M(\epsilon_0)$. We therefore write a simple code that through a linear interpolation for a given input values of the mass M returns the corresponding value of the central density ϵ_0. We remark that of the entire function $M(\epsilon_0)$ was interpolated only the part that allows the formation of stable stars, i.e. where the derivative satisfies

$$\frac{dM}{d\epsilon_0} \geq 0. \tag{4.45}$$

In this region the function $M(\epsilon_0)$ is invertible and therefore the function $\epsilon_0(M)$ is well defined. We are now able to find, given a couple of values m_1 and m_2, the corresponding values of the central density, ϵ_{01} and ϵ_{02} for a given choice of the EOS. We can therefore perform the integration and find a couple of values for the tidal deformabilities Λ_1 and Λ_2.

In figure 4.4 is shown the plot of the values Λ_1 and Λ_2 for each EOS analyzed in this work, overlaid to the data inferred by the detected signals of the neutron stars inspiral.

As we can see from the figure, the equation of state that is mostly favorite by this measures is CBF-EI since is the one that is closest to the region with an higher concentration of the points sampled. The most disfavored is instead the GM3, i.e. the relativistic mean field model. However none of them can be safely excluded since they all are inside the contour of 90% confidence level.

We report also the values of the radius that are predicted by these EOSs for masses belonging to the 90% credible range of the masses measured by the gravitational wave signal GW170817. These values can be confronted with the ones measured in [8] and reported in the previous section. Our results are resumed in table 4.3

If we compare the results of table 4.3 with the values of the radius estimated in [8], previously reported, we find that the only EOS examined that agrees with the

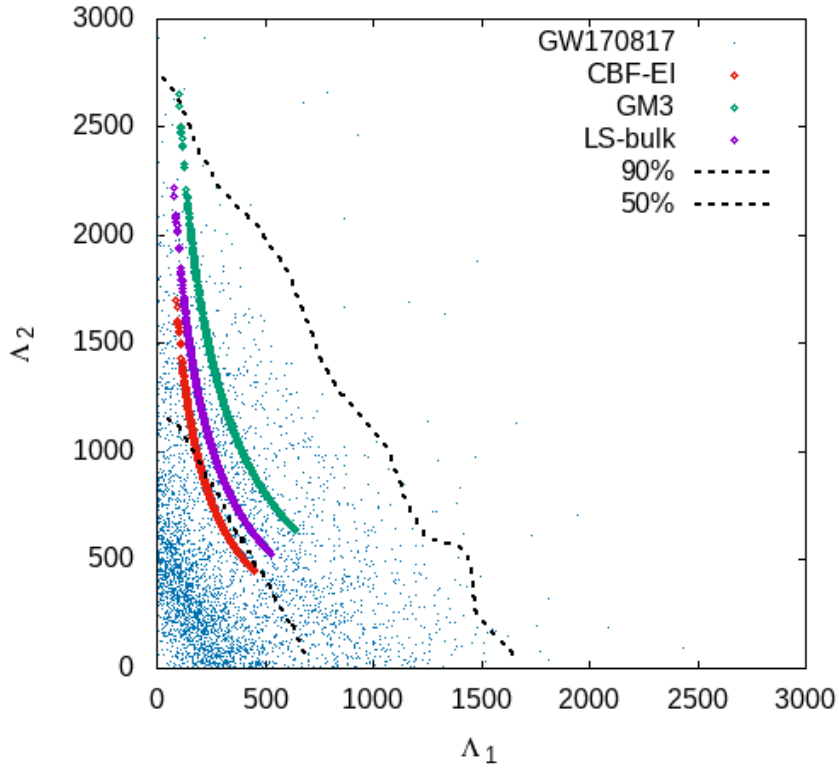

Figure 4.4. Probability density for the tidal deformability parameters inferred by the detected signals of the inspiral of two neutron stars, GW17081027. We overlaid the theoretical predictions obtained within this work for the three EOSs: CBF-EI (red), GM3 (black) and LS-bulk (orange). The dashed lines represent the contours enclosing the 50% and the 90% of the posterior probability density. This contours was read directly from the figure 4.3 (low spin) by means of the program 'xyscan'.

Table 4.3. Table of the radius range, computed with the three EOSs examined in this work, corresponding to the mass range measured by the detected gravitational waves signal.

EOS	$M(M_\odot)$	R(km)
CBF-EI	$1.36 \div 1.60$	$12.52 \div 12.38$
CBF-EI	$1.17 \div 1.36$	$12.61 \div 12.52$
GM3	$1.36 \div 1.60$	$13.24 \div 12.90$
GM3	$1.17 \div 1.36$	$13.43 \div 13.24$
LS-bulk	$1.36 \div 1.60$	$12.82 \div 12.48$
LS-bulk	$1.17 \div 1.36$	$13.00 \div 12.82$

experimental results coming from both the two analysis methods, is the CBF-EI.

Chapter 5

Conclusions

In this work we analyzed three different models for the equation of state of neutron star matter, carrying out the calculation of the relevant astrophysical quantities they affect, by means of the Tolman Oppenheimer and Volkoff (TOV) equations that describe the stellar structure in the framework of general relativity. Within all the relevant astrophysical quantities, this work is mainly focused on the calculation of the tidal Love number, k_2, that is the dimensionless parameter that quantifies the tidal deformation effects induced on a star by an external tidal field. The interest in this quantity is motivated by the recent considerations about the possibility to measure the tidal deformability Λ of a neutron star by means of the gravitational wave signal coming from a binary neutron star (BNS) merger. The tidal deformability is linked to the tidal Love number through

$$\Lambda = \frac{2}{3} k_2 \left(\frac{R}{M} \right)^5 . \tag{5.1}$$

The three EOSs taken into consideration were a mean field one, GM3; one based on the formalism of correlated basis functions within the non relativistic many-body perturbation theory, CBF-EI and a purely phenomenological model, LS-bulk.

In order to solve the TOV equations we revised a numerical integration code, firstly written by Giovanni Camelio, that employs a fourth order Runge-Kutta algorithm. In this code the EOSs is implemented as a tabulated external file that is generated employing a fitting formula firstly described in [6].

We found that the three EOSs predict a maximum values for the mass that is compatible with the heaviest neutron star mass observed to date, i.e. PSRJ0348+0432 with $M = 2.01 \pm 0.04\, M_\odot$. The values that were found in this work are reported in table 5.1.

Table 5.1. Table with the maximum masses for the three EOSs analyzed in this work

EOS	Mass ($M_\odot$)
CBF-EI	2.34
GM3	2.16
LS-bulk	2.02

In chapter 4 we outlined how it is possible to numerical compute the tidal Love number through the integration of the TOV equations. Therefore after we implemented the required modifications to the integration code we computed the tidal deformabilities and the Love number for the three EOSs. We also performed the calculation of the Love number for a set of polytropics with several values of the polytropic index n. These results can be compared with those obtained in [11], with which we found a good agreement. Our results for the Love number calculation are all reported in tables 4.1 and 4.2.

Finally we compared our results with the empirical analysis made in [7] and [8] on the data coming from the gravitational-wave signal detected on 17 August 2017 (GM170817) by the LIGO-VIRGO collaboration.

At this purpose we performed the calculation of the tidal deformability associated with our EOSs, for pairs of stars with masses m_1 and m_2 (with $m_1 \geq m_2$), distributed according to the posterior joint probability distribution found in [7]. We obtained in this way a collection of points in the plot Λ_1 vs. Λ_2 (where Λ_1 and Λ_2 are the two tidal deformabilities associated respectively to the heavier and the lighter star) for each EOS. This prediction can be compared with the analysis made in [7], where they sampled the posterior distribution for Λ_1 and Λ_2 allowed by the shape of the detected waveform. We find that all our EOSs predict values for the pair (Λ_1, Λ_2) that are inside the 90% confidence level given by the posterior probability distribution. However, we can see form the plot shown in figure 4.4, that the experimental data mostly disfavors GM3, while favors CBF-EI.

This last conclusion is also supported by the confrontation between the values of the radius that was found in this work and the ones estimated through [8], employing the LIGO-VIRGO data. Our analysis shows that CBF-EI is the only one EOS that predicts a value of the radius, for star with masses in the range compatible with the observed GW171817, that is in agreement with the one calculated in [8] by means of both the two methods of analysis that the authors have employed.

Appendix

Appendix A

Fitting formula

In this section we will provide the details of the fitting formula for the baryon free energy that was used to evaluate the tabulated EOSs and that was firstly found in [6].

Let us name with f_B the baryon free energy per nucleon. It will be a function of the proton fraction Y_p, the temperature T and the baryon number density n_B (we remember that thanks to the baryon number conservation we can fix the number of baryons). We can split f_B according to

$$f_B(Y_p, T, n_B) = f_B^K(Y_p, T, n_B) + f_B^I(Y_p, T, n_B) \tag{A.1}$$

where K labels the kinetic part and I the interacting part. The kinetic part will be given by classical Fermi gas considerations, we therefore focus our attention on the interacting part of the baryon free energy. In the zero temperature limit the baryon free energy coincides with the baryon energy per nucleon e_B. At zero temperature the baryon energy can be viewed as a function of n_B and of the difference between the fraction of protons and neutrons in the matter, $x = (N - Z)/A$. We can expand $e_B^I(n_B, x)$ around $x = 0$ according to [15]

$$e_B^I(n_B, x) \approx e_B^I(n_B, 0) + S_N(n_B)x^2. \tag{A.2}$$

Where $e_B^I(n_B, 0)$ represent the energy per nucleon of symmetric nuclear matter at density n_B (thus we can call it e_{SNM}^I) while $S_N(n_B)$ is known as the symmetry energy. The previous expansion follows from the experimental observations that symmetric atomic nuclei are more stable than the others, therefore the point $x = 0$ must be a stationary point for the function $e_B^I(n_B, x)$ for fixed n_B. We can also define the energy of the pure neutron matter, i.e. nuclear matter without protons, as

$$e_{\mathrm{PNM}}^I(n_B) = e_B^I(n_B, 1) \approx e_{\mathrm{SNM}}^I(n_B) + S_N(n_B). \tag{A.3}$$

If we remember that $x = 1 - 2Y_p$, joining together (A.2) and (A.3) yields

$$\begin{aligned} e_B^I(Y_p, T = 0) &\approx e_{\mathrm{SNM}}^I + \left(e_{\mathrm{PNM}}^I - e_{\mathrm{SNM}}^I\right)(1 - 2Y_p)^2 \\ &= 4Y_p(1 - Y_p)e_{\mathrm{SNM}}^I + (1 - 2Y_p)^2 e_{\mathrm{PNM}}^I, \end{aligned} \tag{A.4}$$

where the dependence on n_B is understood.

In [6] it is assumed that finite temperature effects do not change the Y_p dependence of the baryon free energy, which therefore assumes the form

$$f_B^I(Y_p, n_B, T) = 4Y_p(1-Y_p)f_{\rm SNM}^I(n_B, T) + (1-2Y_p)^2 f_{\rm PNM}^I(n_B, T). \tag{A.5}$$

The quantities of interest are now $f_{\rm PNM}^I(n_B, T)$ and $f_{\rm SNM}^I(n_B, T)$.

A good fitting formula for the free energy needs continuity of the second derivatives and the following constraints to be satisfied: (i) $s \to 0$ as $T \to 0$, (ii) $f_B^I \to 0$, $s_B^I \to 0$, $P_B^I \to 0$ as $n_B \to 0$. They find that under these requirements, a good compromise between the number of parameters and the precision of the fit is given by the following polynomial fitting formula:

$$\begin{aligned} f_j^I(n_B, T) = {} & a_{1,j} n_B + a_{2,j} n_B^2 + a_{3,j} n_B^3 + a_{4,j} n_B^4 + \\ & + n_B T^2 (a_{5,j} + a_{6,j} T + a_{7,j} n_B + a_{8,j} n_B T), \end{aligned} \tag{A.6}$$

where $j = \{\text{SNM; PNM}\}$. The fit with the formula given by putting together (A.5) and (A.6) was performed on the EOSs GM3 and CBF-EI. The values of the coefficients that were used for the fit are reported in table A.1. For the LS-bulk EOS it was used the analytical expression given by

$$f_B^I = \left[a + 4bY_p(1-Y_p)\right] n_B + c n_B^\delta - Y_p \Delta_m, \tag{A.7}$$

with

$$\begin{aligned} \delta &= 1.260 \\ a &= -711.0\, MeV\, fm^3 \\ b &= -107.1\, MeV\, fm^3 \\ c &= 934.6\, MeV\, fm^{3\delta} \\ \Delta_m &= 0\, MeV. \end{aligned} \tag{A.8}$$

We finally remark that though this formula accounts for finite temperature scenarios, in our work we always take in consideration the $T = 0$ case.

Table A.1. Table with the values of the fitting coefficients employed for the two EOSs GM3 and CBF-EI.

Coefficient	GM3	CBF-EI
$a_{1,\mathrm{SNM}}$	-402.401	-284.592
$a_{2,\mathrm{SNM}}$	1290.54	676.121
$a_{3,\mathrm{SNM}}$	-1540.52	-662.847
$a_{4,\mathrm{SNM}}$	903.8	667.492
$a_{5,\mathrm{SNM}}$	0.0669357	0.112911
$a_{6,\mathrm{SNM}}$	-0.000680098	-0.00124098
$a_{7,\mathrm{SNM}}$	-0.0769298	-0.148538
$a_{8,\mathrm{SNM}}$	0.000915968	0.00192405
$a_{1,\mathrm{PNM}}$	-274.544	-121.362
$a_{2,\mathrm{PNM}}$	1368.86	101.948
$a_{3,\mathrm{PNM}}$	-1609.15	1079.08
$a_{4,\mathrm{PNM}}$	916.956	-924.248
$a_{5,\mathrm{PNM}}$	0.0464766	0.0579368
$a_{6,\mathrm{PNM}}$	-0.000388966	-0.000495044
$a_{7,\mathrm{PNM}}$	-0.0572916	-0.0729861
$a_{8,\mathrm{PNM}}$	0.00055403	0.000749914

Bibliography

[1] Ian Harry and Tanja Hinderer. Observing and measuring the neutron-star equation-of-state in spinning binary neutron star systems. *Classical and Quantum Gravity*, 35(14):145010, 2018.

[2] Valeria Ferrari. Lecture notes for the master's degree courses: "Relatività Generale" and "Onde gravitazionali, stelle e buchi neri".

[3] N.W. Ashcroft and N.D. Mermin. *Solid State Physics*. Saunders College, Philadelphia, 1976.

[4] Omar Benhar Noccioli. The structure of compact stars, 2017. Lecture notes for the XXXII cicle of Physics PhD.

[5] Omar Benhar and Alessandro Lovato. Perturbation theory of nuclear matter with a microscopic effective interaction. *Phys. Rev. C*, 96:054301, Nov 2017.

[6] Giovanni Camelio, Alessandro Lovato, Leonardo Gualtieri, Omar Benhar, José A. Pons, and Valeria Ferrari. Evolution of a proto-neutron star with a nuclear many-body equation of state: Neutrino luminosity and gravitational wave frequencies. *Phys. Rev. D*, 96:043015, Aug 2017.

[7] B. P. Abbott *et al.* (LIGO Scientific Collaboration and Virgo Collaboration). Gw170817: Observation of gravitational waves from a binary neutron star inspiral. *Phys. Rev. Lett.*, 119:161101, Oct 2017.

[8] The LIGO Scientific Collaboration and the Virgo Collaboration. Gw170817: Measurements of neutron star radii and equation of state. *Phys. Rev. Lett.*, 121:161101, Oct 2018.

[9] Carl D. Murray and Stanley F. Dermott. *Solar System Dynamics*. Cambridge University Press, 2000.

[10] Taylor Binnington and Eric Poisson. Relativistic theory of tidal love numbers. *Phys. Rev. D*, 80:084018, Oct 2009.

[11] Tanja Hinderer. Tidal love numbers of neutron stars. *The Astrophysical Journal*, 677(2):1216, 2008.

[12] Tanja Hinderer, Benjamin D. Lackey, Ryan N. Lang, and Jocelyn S. Read. Tidal deformability of neutron stars with realistic equations of state and their gravitational wave signatures in binary inspiral. *Phys. Rev. D*, 81:123016, Jun 2010.

[13] Thorne K. S. Campolattaro A. Non-radial pulsation of general-relativistic stellar models. i. analytic analysis for l >= 2. *ApJ*, 149:591, sep 1967.

[14] Milton Abramowitz and Irene A. Stegun. *Handbook of Mathematical Functions with Formulas, Graphs, and Mathematical Tables*. Dover, New York, ninth dover printing, tenth gpo printing edition, 1964.

[15] M. Baldo and G.F. Burgio. The nuclear symmetry energy. *Progress in Particle and Nuclear Physics*, 91:203 – 258, 2016.